Barometer Coefficients of High Latitude Neutron Monitors

Masahiko KUSUNOSE
Department of Information Science, Faculty of Science
Kochi University, Kochi 780, Japan

Abstract: The cosmic ray monitor is used to measure the primary cosmic ray intensity. The counting rate of neutron monitor is affected by the atmospheric pressure variation. The amplitude of the variation in the counting rate caused by the atmospheric pressure is usually larger than that of the primary cosmic ray intensity. It is very important to derive a certain appropriate barometer coefficient to make a reliable correction of the counting rate for the barometric pressure. To decide the barometer coefficients of the neutron monitors, it is necessary to separate the intensity variations caused by the primary cosmic ray itself and that due to the pressure variation. To this end, we adopted the spherical harmonic analysis using the neutron monitor data from about twenty stations located in the high latitude region where the geomagnetic cutoff rigidity is below 2.3 GV. The primary cosmic ray variations are removed from the observed data, and thus the residuals are derived. Through the study of the correlations between the derived residual and the daily mean pressures, reevaluation of the barometer coefficients was made by using twelve-years data from January 1966 to December 1977. The re-evaluated barometer coefficients for every year were tabulated. The result shows that the re-evaluated barometer coefficients at a few stations are considerably deviated from the conventionally used coefficients. Further analysis is made on the data observed at the selected eight stations, where complete twelve-years data were available. As a result, it is found that the long-term variation of the revised barometer coefficients is correlated in positive sense with that of the cosmic ray neutron intensity levels. The barometer coefficient depends on the cosmic ray neutron intensity. The dependence in the solar quiet period is stronger than that in the solar active period. Using the rigidity spectrum of the barometer coefficient and the cosmic ray neutron intensity at sea level, the dependence of the barometer coefficient on the primary spectrum variation was estimated by numerical calculation.

The result shows clearly that the variation rate of the barometer coefficient against the cosmic ray neutron intensity is influenced by the changes in the cutoff rigidity and in the primary spectrum.

Key words : Cosmic Ray, Neutron Monitor, Barometer Coefficient.

1. Introduction

In general, cosmic radiations are classified into two components : primary and secondary.

Most of the primary cosmic rays are the galactic cosmic rays arriving onthe top of the earth's atmosphere from outside the earth, while the secondary ones are those produced in the air through nuclear interactions between the primary cosmic rays and air nuclei. It is well known that most parts of the primary cosmic ray particles whose highest energy amounts to the order of 10^{22} eV have their origins in the universe outside the solar system and a little contribution from the sun is recognized as the so-called solar cosmic rays with energies of the order of 10^{9} eV.

On the travelling journey of the primary cosmic ray particles from the outside of the solar system toward the earth, they usually suffer from various kinds of modulations such as scattering, degradation and deflection owing to the ordered or disordered interplanetary magnetic field as well as the earth's magnetic field. As a result, cosmic ray intensity variations observed on the earth are influenced by several types of modulations.

Time modulations of the primary cosmic ray intensity include the transient and long-term variations. The former is the Forbush decrease, solar cosmic ray event, diurnal variations and so on. The latter is the periodical fluctuations caused by the rotation of the sun and the eleven-year solar activity change. These two kinds of modulations can be detected easily on the earth's surface. When we observe the cosmic ray intensity by the neutron monitor on the ground, the atmospheric and temperature effects on the secondary cosmic rays are usually superposed on the primary cosmic ray modulations. It is very important to discriminate the primary and secondary modulations as precisely as possible, to show characteristics of the respective modulations.

Since the primary cosmic ray modulations are concerned with three dimensional anisotorpic flows of cosmic ray particles in space, the spherical harmonic analysis is one of the most useful methods to understand the physical characters of the modulations. For example, this analysis was applied by Yoshida *et al.* (1971) to the studies of the Forbush decrease and also by Nagashima (1971) to the solar and sidereal anisotropies. For these studies are essential the data from a network of cosmic ray stations distributed uniformly over the globe.

In the earlier stage of cosmic ray modulation studies, continuous monitoring of the secondary cosmic ray intensity had started by using the ionization chamber that is one of the most simple and stable instruments to detect the cosmic ray muon component. After that the precision ionization chamber was developed by Compton *et al.* (1934) and four sets of the identical chambers were installed at four different stations:
Huancayo, Cheltenham, Christchurch and Godhavn. In Japan, five sets of the Nishina-type ionization chambers had been constructed for the aim of establishing a similar network system of observations during the period 1934 - 1941 (Ishii, 1944). Four Compton-type and one Nishina-type of chambers have been in satisfactory operation for more than 40 years (Kusunose and Wada, 1969). Muon data accumulated during such long period are useful for the studies of the 11-year solar cycle modulations.

Muon observations were further extended to a new technique of multi- directional telescopes using plural arrays of the Geiger-Müuller counters and/or plastic scintillation counters. This observation method has made possible not only improvement of the

statistical accuracy but also directional surveys of modulations in space at a station.

Another important component of the secondary cosmic rays is the nucleonic component that has the energy response to the primary cosmic rays different from that of the muon component and it has little effect of the atmospheric temperature. Simpson (1957) developed the first standardized device for measuring this component, which is called the IGY-type (International Geophysical Year, 1957 - 1958) of neutron monitors and has been in operation throughout the world. The data obtained by this device are now widely used by many cosmic ray investigators through the World Data Centers for Cosmic Rays.

Cosmic ray neutron data obtained by the neutron monitor have been highly evaluated by improving the IGY-type into the IQSY-type (International Quiet Sun Year, 1964 - 1965) using the large neutron counter with detection sensitivity increasing by an order of magnitude higher than that of IGY neutron counter (Carmichael, 1964). The number of IQSY neutron monitors being now in operation amounts to about fifty.

Fluxes of cosmic ray nucleonic component are modulated in the atmosphere. Counting rates of the ground-based neutron monitor are very sensitive to the atmospheric pressure variations, therefore the monitor seems to be a kind of barometer. As is shown in Fig. 1, the amplitude of neutron intensity variations due to pressure variations exceeds usually the primary cosmic ray intensity variations, except in cases of the Forbush decrease and the

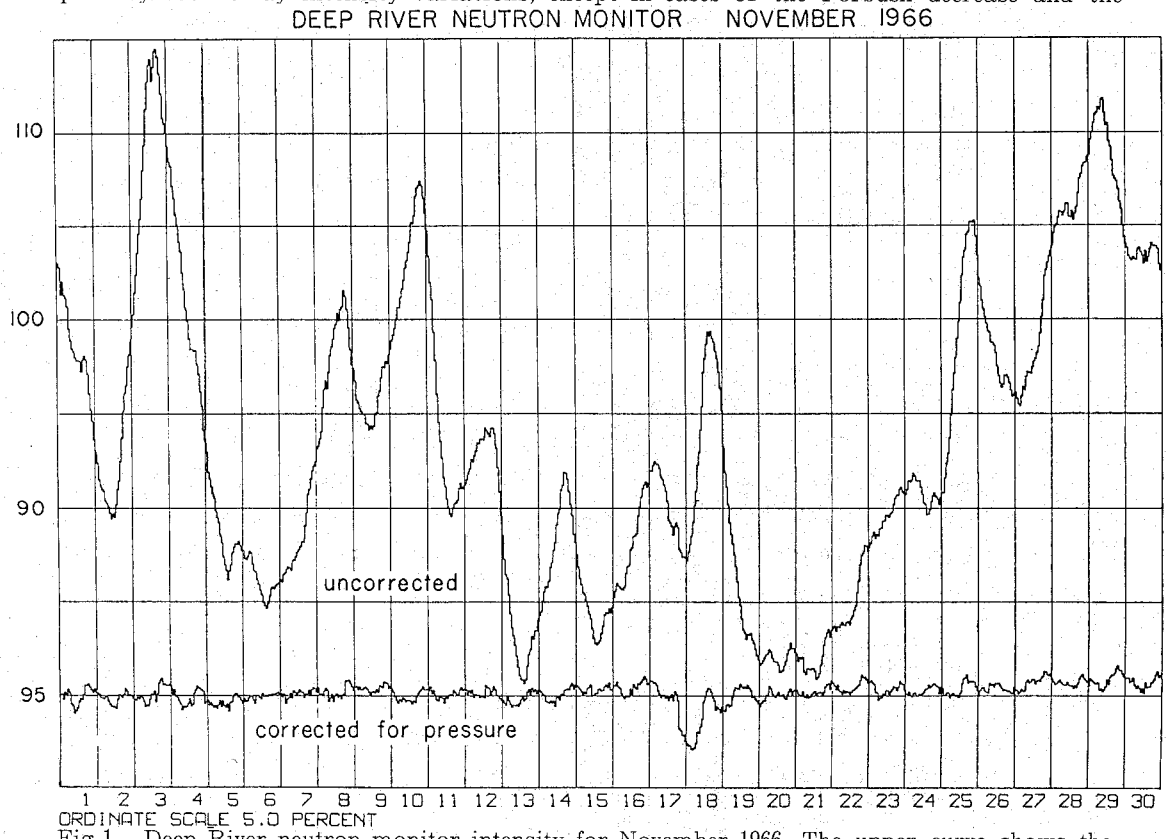

Fig.1. Deep River neutron monitor intensity for November 1966. The upper curve shows the intensity before correction, the lower curve, the intensity after correction foratmospheric pressure and temperature. (Bercovitch, 1967).

solar cosmic ray increase. Therefore the correction of the observed neutron intensity variations for the pressure variations must be made as carefully as possible, when we use the neutron data for modulation studies of the primary cosmic ray intensity. Namely the barometer coefficient to be used in the correction procedure must be estimated accurately.

In this article, we had first tried to re-examine whether the reported barometer coefficients of the existing neutron monitors are reliable or not. As described above, it is important to separate between the atmospheric effects of the secondary cosmic rays and the primary cosmic ray modulation as completely as possible. To do this, the spherical harmonic analysis was applied by using neutron monitor data from about twenty stations located at high latitudes where the vertical cutoff rigidity is below 2.3 GV. The reason why high-latitude stations were selected here is that their cutoff rigidity is close to the cutoff value by the atmosphere. Their mean effective rigidity is estimated to be about 9.5 GV (Nagashima *et al*, 1968). Neutron monitor data have been taken over twelve years from January 1966 to December 1977. Re-evaluation of the barometer coefficients was made for every year, giving the revised coefficients for several stations.

Next we investigated the solar cycle dependence of the revised barometer coefficients. An accurate knowledge of the solar cycle variation of the barometer coefficient is essential in order to correct properly the station data for the changes in the local barometric pressure. There are several studies on this subject (for instance Kamphouse, 1963; Forman, 1965; Griffiths *et al.*, 1966; Bachelet *et al.*, 1972; Raubenheimer and Stoker, 1974), but our results show more fine aspect of variation than previous works.

Lastly we studied the relation between the barometer coefficient of high latitude neutron monitor and the primary cosmic ray variation spectrum through the theoretical analysis and numerical calculations.

2. Neutron Monitor

The neutron monitor is a device that detects the cosmic ray nucleon component; it consists of an array of BF_3 proportional counters surrounded by double layers of lead and polyethylene (or paraffin). The neutron monitor indeed measures secondary neutrons produced locally by nuclear interactions between the nucleonic component and lead nuclei. It is important to exclude environmental background neutrons produced in the surrounding materials outside the monitor by the polyethylene shield that contains a high percentage of hydrogen nuclei.

2.1. BF_3 proportional counter

A BF_3 proportional counter is filled with boron trifluoride BF_3 gas in which boron content is enriched to 96%^{10}B (Hatton, 1971). A neutron that is captured by a ^{10}B nucleus induces the exothermic reaction:

$$^{10}_{5}B+^{1}_{0}n \rightarrow ^{7}_{3}Li+^{4}_{2}He \qquad (2.1)$$

The neutron capture cross section of this reaction obeys $1/v$-law (v : velocity of

neutron), being ~ 3820 barns (1 barn = $10^{-28}m^2$) at thermal energies (1/40eV). As the counter is operated in the proportional region, it is easy to discriminate large pulses caused by $^4_2$He nucleus from somewhat small pulses produced by muons, electrons or gamma rays passing through this counter. Alpha pulses thus detected have one-to-one correspondence to incident nucleons.

Around each counter there is an inner moderator, the function of which is to slow down fast neutrons to near thermal energies to facilitate their capture in the boron trifluoride. Surrounding the inner moderator, there is the producer in which the evaporation neutrons are produced. Besides, the entire device is enclosed by a reflector that reflects the neutrons also moderates them. The reflector has the additional function of absorbing and reflecting unwanted low energy neutrons produced in the atmosphere and in materials close to the monitor.

2.2. The IGY and NM64 monitor

As shown in Fig. 2, a full size of the standard IGY type neutron monitor contains 12 counters and usually is divided into a duplicate unit consisting of six counters each. The total counting rates of the monitor is ~ 24,000 counts/hour at a high-latitude sea level

Table 1. Comparison of the dimensions and counting rates of various cosmic ray neutron monitor designs. (Hatton, 1971)

	Standard IGY	leeds IGY	Ottawa	NM64
Number of counters per channel	6	6	1	6
Counters				
Active length(cm)	86.4	41	69	191
Diameter(cm)	3.8	5.1	6.35	14.8
Pressure(cm Hg)	45	40	56	20
Inner moderator				
Average thickness(cm)	3.2	3.3	5.4	2.0
Producer				
Average depth(g cm^{-2})	153	153	285	156
Area per channel(m^2)	0.94	0.72	0.17	6.21
Length parallel to counters(cm)	102	76	61	207
Reflector				
Average thickness(cm)	28	28	13	7.5
*Counting rate(1962)**				
Of a high latitude sea-level station				
Per channel per hour	~12000	~ 9000	~ 6000	~250000
Per m^2 of producer	~12800	~12000	~35000	~ 40000

* The counting in 1962 has been adopted as representative of the average counting rate over the solar cycle.

station. Dimensions of various types of the neutron monitors are summarized in Table 1.

A radical change took place in the design of neutron monitors from the need for a much larger counting rate the order of 10^6 counts/hour or greater), which leads to the improved statistical accuracy of neutron monitor data. The NM64 monitor was designed (Carmichael, 1964) by using large (BP28) BF_3 proportional counters developed by Fowler(1963). Figure 2 shows its geometry. The quantity of ^{10}B in the effective volume of each counter should be approximately 2.1×10^{23} atoms.

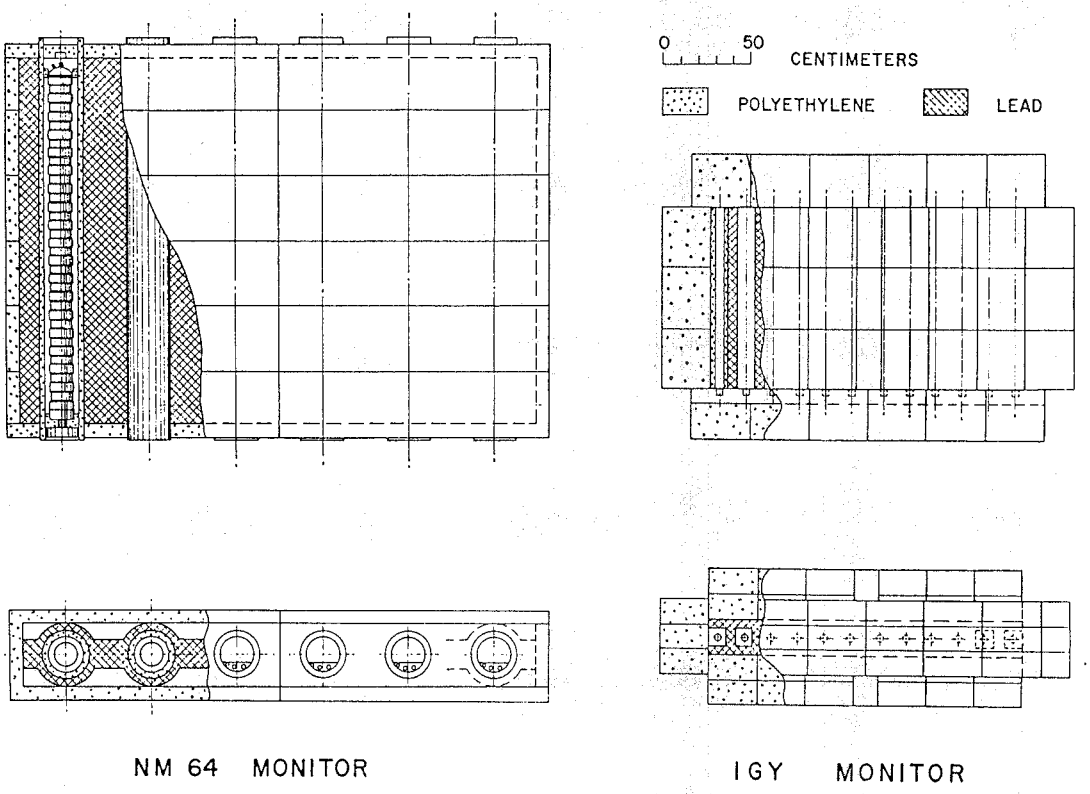

Fig.2. Plans and elevations of a six-counter unit of NM64 neutron monitor and of a twelve-counter unit of IGY neutron monitor. Incident nuclear particles interact with the lead target yielding evaporation neutrons that are moderated in the inner polyethylene sheath (paraffin for IGY) and captured in the gas of the counters. The drawings show the structure of the NM64 and IGY neutron monitors on the same scale.
(IGY: Simpson, 1957 and NM64: Carmichael, 1964).

An innovation in the NM64 monitor design was the use of polyethylene in place of paraffin as the inner moderator. This alternation enabled the counter with a moderator to be manufactured as a single assembly. Paraffin wax and polyethylene are both composed of carbon and hydrogen, and essentially the carbon-hydrogen ratios are the same. The use of polyethylene reflector has also been able to make a convenient installation that the producer of lead could be placed directly on the lower portion of reflector. A full-size of NM64 neutron monitor consist of 18 counters separating to three units containing six

counters each. The counting rate of one unit of 18-NM64 is ~ 750,000 counts/hour at a high latitude sea level station.

2.3. Multiplicity and total counting rate

Multiplicity means the number of neutrons produced in a single nuclear reaction. Cosmic ray nucleus interacting in the lead producer of the neutron monitor result in the multiproduction of evaporated neutrons within the short time interval of about 1 μ sec.

The total counting rate N is given by the product of the intensity I, the interaction probability P, the mean multiplicity of neutrons $\bar{m}$, and the detection probability ϵ. Thus

$$N = IP\bar{m}\epsilon A, \tag{2.2}$$

where A is the effective area of the lead in the monitor.

Multiplicity measurements have been performed for the IGY neutron monitor (Bachelet *et al.*, 1964, 1965; Kent *et al.*, 1968; Dyring and Sporre, 1966a, 1966b) and the NM-64 neutron monitor (Griffiths *et al.*, 1968; Blomster and Tanskanen, 1969;Agrawal *et al.*, 1969; Smirnov and Ustinovitch, 1969;Lockwood and Singh, 1969).

Hughes and Marsden (1966) suggested that the detected multiplicity spectrum would reflect the energy dependence of the primary cosmic radiation. The spectral response functions were determined experimentally by latitude surveys carried out at different phase of solar cycle (Kodama and Inoue, 1969).

The neutron multiplicity distribution depends upon the geometry of the neutron monitor, for instance, the arrangement of the monitor pile, or the number of operated neutron counters (Hatton and Carmichael, 1964; Fujii *et al.*, 1972).

According to Kodama and Inoue (1970), it is known that the barometer coefficients and the magnitudes of intensity variations as observed in the solar proton and Forbush decrease events are decreasing with the increasing multiplicity, while no significant multiplicity effect is recognized in the diurnal variation.

It is expected that the time variations in the rates of the detected multiplicities will reflect the characteristics of the primary energy spectrum of the cosmic radiation, and then this matter will be useful in the study of the various time-dependent phenomena of the cosmic ray.

2.4. Contributions made by the various components

Cosmic ray neutron monitors are sensitive to the secondary components of the nucleon cascade, which are generated in nuclear interactions throughout the atmosphere. Many authors have made the quantitative estimations of the contributions of the secondary components to the total counting rates obtained by the neutron monitor (Simpson *et al.*, 1953; Hughes and Marsden, 1966).

Hatton (1971) made a certain significant improvement on the calculations of Harman and Hatton (1968) to incorporate more recent data of the various parameters required. The results are given in Table 2 for both the IGY and NM64 monitors, where the fractional

counting rate of a neutron counter is in general due to secondary neutrons, protons, muons captured in the detector. The daily counting rate from each component, N_i, was calculated under the assumption that the various components make the same fractional contribution to the interactions in the moderator and surroundings as that in the producer.

The contributions made by the various components are found to be comparable for the two monitors, although those are not identical. In addition, because the uncertainties in those contributions are not independent for the two monitors, the differences are important and may be interpreted in terms of the reduced reflector thickness in the NM64 monitor.

Table 2. The contributions made by secondary components to the counting rate of the IGY and NM64 monitors. (Hatton, 1971)

Component	IGY monitor		NM64 monitor	
	Daily counting rate	% Contribution	Daily counting rate	% Contribution
Neutrons	161200	83.6±2	4857000	85.2±2
Protons	15200	7.4±1.0	423000	7.2±1.0
Pions	2530	1.2±0.3	58000	1.0±0.3
Stopping muons	9150	4.4±0.8	212000	3.6±0.7
Interacting muons	4800	2.4±0.4	118000	2.0±0.4
Background	2000	1.0	60000	1.0
Predicted total	194880		5728000	
Observed total	216000		6000000	

The contributions given in Table 2 are applied to a high latitude sea-level station with a thin roof above the monitor. It may be expected that they will vary slightly at individual stations depending upon the thickness and material of the roof. They are also average values for the solar cycle. During the 1954-65 solar cycle the total intensity of a high latitude sea-level neutron monitor decreased by ~18% while that of a muon monitor decreased by ~ 5%.

3. Spherical Harmonic Analysis

As a first approximation the external magnetic field of the earth can be represented by a dipole located in the center of the earth. The first geophysical application of the spherical harmonic analysis was Gauss's analysis of the potential of geomagnetic dipole field (Gauss, 1839), and since then spherical harmonic analysis has been used for various studies that must represent geophysical quantities as functions of spherical coordinates. In the present section, the spherical harmonic analysis is applied to the cosmic ray intensity variations observed by the worldwide network of ground based neutron monitors.

3.1. Cutoff rigidity

A charged particle is characterized by the rigidity $R=pc/Ze$, where Ze is the charge and p the momentum of a particle, and c the velocity of light. The rigidity R is usually expressed in unit of [GV]. It has been shown by Störmer (1955) that particles with any rigidity less than a critical value R_c (cutoff rigidity), are unable to reach a specific point on the earth's surface. The cutoff rigidity R_c is given by

$$R_c = \frac{M}{4r_e^2}\cos^4\theta\,, \tag{3.1}$$

where r_e is the radius of the earth, θ the geomagnetic latitude of the point and M the dipole moment of the spherical harmonic expansion of the magnetic potential of the earth.

To have a full knowledge of the cutoff rigidities at different geographic locations on the earth is of great importance in the study of the energy spectrum and modulations of primary cosmic ray intensity.

3.2. Asymptotic directions of approach

Information about the directions of propagation of a cosmic ray particle in the interplanetary space before they enter to the vicinity of the geomagnetic field is required for the study of the spatial dependence of primary cosmic rays. The cosmic ray particles that arrive at any point on the earth's surface have been deflected in the geomagnetic field. To relate the time variations of cosmic ray intensities observed on the ground to the time variations and anisotropy of the primary cosmic rays in the interplanetary space, it is essential for the analysis of the data to take into account these deflections.

Suppose that cosmic ray particles having a rigidity R arrives from the vertical direction, in average, at a location on the earth surface, where the geographic latitude and longitude are φ, and λ respectively. Those cosmic ray particles are deflected in the geomagnetic field as shown in Fig. 3. Let us refer the direction of approach before their entering into

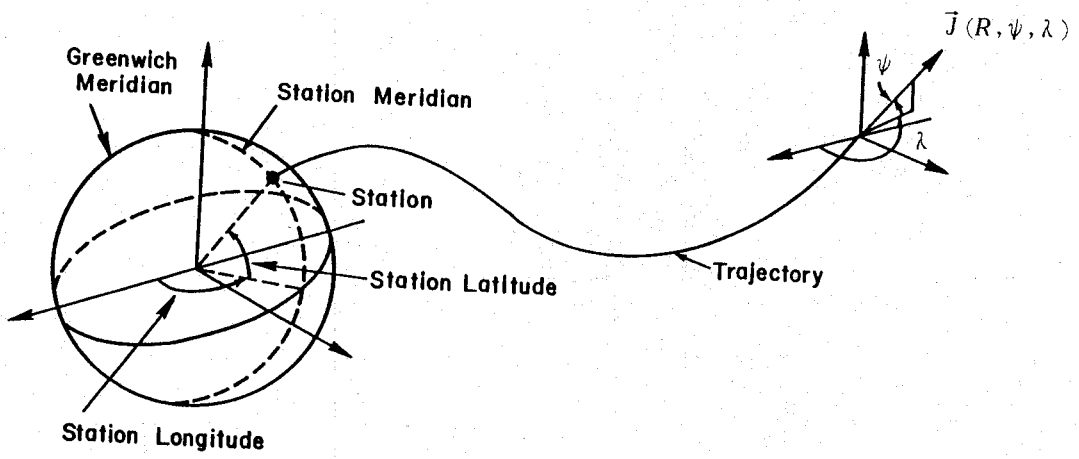

Fig.3. The trajectory of a charged particle through the geomagnetic field. Illustration of the definition of the asymptotic direction of approach. (McCracken *et al.*, 1965).

the geomagnetic field to as the asymptotic direction of approach $\vec{J}, R, \varphi, \lambda$. This direction suggests the direction of motion in the interplanetary space of a cosmic ray that is able to arrive eventually at a position (φ, λ) on the earth surface typically from the vertical direction.

Since there are no analytic expressions for the asymptoic directions except the special case. Therefore, the derivation of the asymptotic directions has been possible only either by model experiments, in which a small model of the earth and its field is used to experimentally simulate the actual physical situation, or by numerical integration of the equations of motion of cosmic ray particles. The former method has been developed by Malmfors (1945), and Brunberg and Datner (1953), while the latter has been investigated by Störmer (1955), Jory (1956), and Lust and Simpson (1957).

The orbit of a negatively charged particle moving outward from a specific location on the earth is identical with the orbit of a positive particle of equal rigidity approaching the earth from the outside and ultimately arriving at the same location. Programs and methods that use the differential equation of motion

$$m\frac{d^2\vec{r}}{dt^2} = q\frac{d\vec{r}}{dt}\times\vec{B} \tag{3.2}$$

to decide the path of a particle of charge q and mass m in the earth's magnetic field $\vec{B}$ by numerical integration, have been published by many authors (Inoue it *et al.*, 1983, and the references there in). In the present work, two tables of the asymptotic directions, mainly in the epoch of 1955 (McCracken it *et al.*, 1965) and partly the epoch of 1975 (Inoue *it et* al., 1983) were used.

3.3. Method of the spherical harmonic analysis

Here, we describe the method of analysis according to Yoshida it *et al.* (1971). A function $f(\theta, \varphi)$ defined on a spherical surface in terms of the polar coordinates θ and φ, as shown in Fig. 4, is expanded into a series of the spherical harmonic functions as

$$f(\theta, \varphi) = \sum_{l=0}^{\infty} Y_l(\theta, \varphi) \tag{3.3}$$

where

$$Y_l(\theta, \varphi) = C_l P_l(\theta, \varphi) + \sum_{m=1}^{l} \{A_l^{(m)} \cos m\varphi + A_l^{(m)} \sin m\varphi\} P_l^{(m)} \cos\theta). \tag{3.4}$$

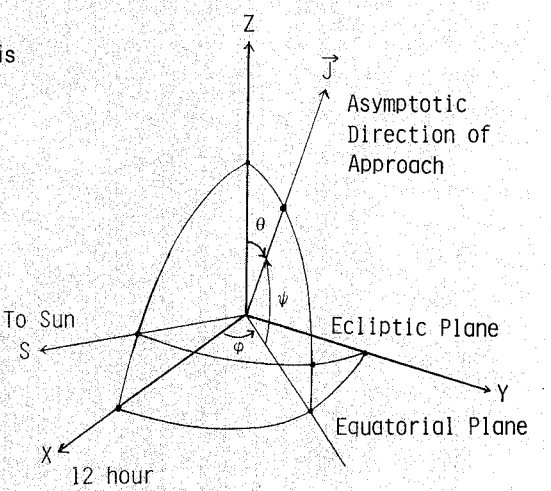

Fig.4. Equatorial and ecliptic coordinate systems.
Z:Equatorial north pole
S:Direction of the sun
$\vec{J}$:Direction of incident particle
ϕ, ψ and θ:geographic longitude, latitude and co-latitude

In the above equation, $A_l^{(m)}$, $B_l^{(m)}$, and C_l are harmonic coefficients. The sum of the terms up to the second order of $l=2$, is given as

$$Y(\theta, \varphi) = \sum_{l=0}^{2} Y_l(\theta, \varphi), \tag{3.5}$$

where

$$Y_0(\theta, \varphi) = C_0 P_0 \cos\theta, \tag{3.5a}$$

$$Y_1(\theta, \varphi) = C_1 P_1(\cos\theta) + (A_1^{(1)} \cos\varphi + B_1^{(1)} \sin m\varphi) P_1^1(\cos\theta), \tag{3.5b}$$

$$Y_2(\theta, \varphi) = C_2 P_2(\cos\theta) + (A_2^{(1)} \cos\varphi + B_2^{(1)} \sin m\varphi) P_2^1(\cos\theta) + (A_2^{(2)} \cos 2\varphi + B_2^{(2)} \sin 2\varphi) P_2^2(\cos\theta). \tag{3.5c}$$

Further, the associated Legendre functions $P_l^m(\cos\theta)$ up to the order of l, $m = 0, 1, 2$ are expressed as in the next table, where $l \geq m$ and $P_l(\cos\theta) = P_l^0(\cos\theta)$.

l/m	Isotropic/zonal component 0	First harmonic component 1	Second harmonic component 2
0	1		
1	$\cos\theta$	$\sin\theta$	
2	$\frac{1}{2}(\cos^2\theta - 1)$	$3\sin\theta\cos\theta$	$3\sin^2\theta$

Now, we express the asymptotic direction of the i-th station specified by the polar coordinates θ_i and φ_i, which are given with respect to the earth's axis and the direction toward the sun, respectively. As shown in Fig. 4 and Fig. 5, the polar coordinates (θ_i, φ_i) are related to the asymptotic latitude φ_i and longitude λ_i as follows:

$$\theta_i = \pi/2 - \varphi_i \text{ and } \varphi_i = \omega(t-12) + \lambda_i \tag{3.6}$$

where t denotes UT (Universal Time), and ω is the angle velocity of the earth's self rotation ($\omega = \pi/12$rad/hour).

Nine harmonic coefficients up to the second order, C_0, C_1, C_2, $A_1^{(1)}$, $B_1^{(1)}$, $A_2^{(1)}$, $B_2^{(1)}$, $A_2^{(2)}$ and $B_2^{(2)}$ are determined every one hour from the data of cosmic ray intensities $I(\theta_i, \varphi_i)$ at stations, where $i = 1, 2, 3, \cdots, n$, by the least square fitting method, which is to minimize

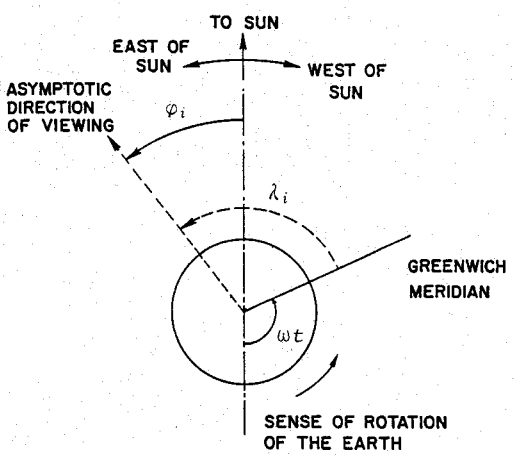

$$\varphi_i = \omega(t-12) + \lambda_i$$

Fig.5. Defining the angles employed to specify theasymptotic direction of viewing an arbitrarstation.

minimize the total sums of square deviations weighted by, W_i's

$$S=\sum_{i=1}^{n} W_i[I(\theta_i, \varphi_i)-Y(\theta_i, \varphi_i)]^2 \tag{3.7}$$

where the mean counting rate at an i-th station is given by W_i and n is the number of stations.

The coefficient $C_0(t)$ is the isotropic (worldwide) component, and $C_1(t)$, together with $A_1^{(1)}(t)$ and $B_1^{(1)}$, (after thisabbreviated as A_1 and B_1) constitutes the first order of anisotropic component. The coefficient C_1 gives the amplitude of the north-south asymmetric (latitudinal) component and the quantity $(A_1^2+B_1^2)^{1/2}$ gives that of the longitudinal asymmetry. The maximum flux of cosmic rays represented by the first harmonic terms comes from the asymptotic longitude given by

$$\Phi=\tan^{-1}(B_1/A_1). \tag{3.8}$$

One also can define the three dimensional quantities,

$$P=(A_1^2+B_1^2+C_1^2)^{1/2}, \tag{3.9}$$

$$\Psi=\tan^{-1}\{C_1/(A_1^2+B_1^2)^{1/2}\}. \tag{3.10}$$

The quantity P gives the maximum anisotropic component flux that appears in an asymptotic direction specified by the geographic latitude Ψ and longitude Φ. These relations are illustrated in Fig. 6.

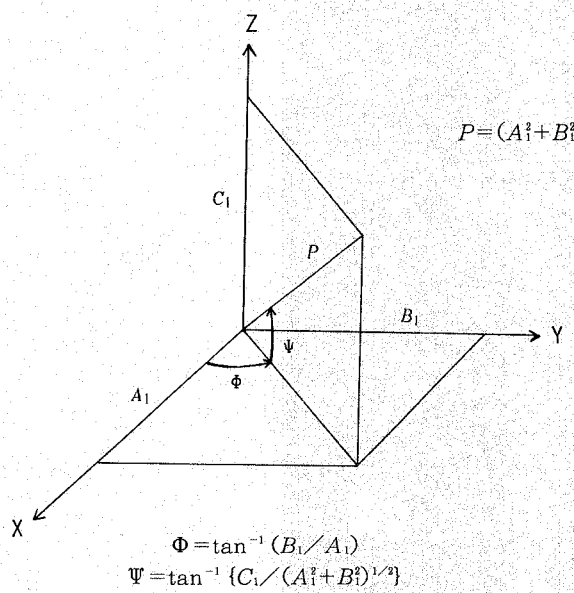

Fig.6. Illustration of coefficients A_1, B_1, C_1 and P that give the maximum anisotropic component flux, which appears in an asymptotic direction given by the geographical latitude Ψ and longitude Φ.

The stations where data are used in the analysis are given in Table 3. For each station, the vertical cutoff rigidity, the asymptotic direction (φ_i and λ_i), and the mean counting rates (W_i) are given. The vertical cutoff rigidities for every station can be seen to be less than 2.3 GV, which is close to the atmospheric cutoff value. The geographic distribution of the stations is shown in Fig. 7.

It is assumed as the first approximation that the mean rigidity of primary cosmic ray particles arriving at every station is almost equal to 9.5 GV. This assumption is based on the fact that the effective asymptotic latitudes obtained for 11 stations (except for Sulphur Mt.) agree within accuracy of $\pm 5°$ with the asymptotic latitudes obtained by McCracken it *et al.* (1965) for the rigidity value of 9.5 GV (Nagashima it et *al.*, 1968).

Figure 8 shows the geographic distribution of the asymptotic directions for rigidity 9.5 GV at UT=0 for all the stations where data are used in this analysis. A geographically uniform distribution of stations is essential for making an accurate spherical harmonic analysis.

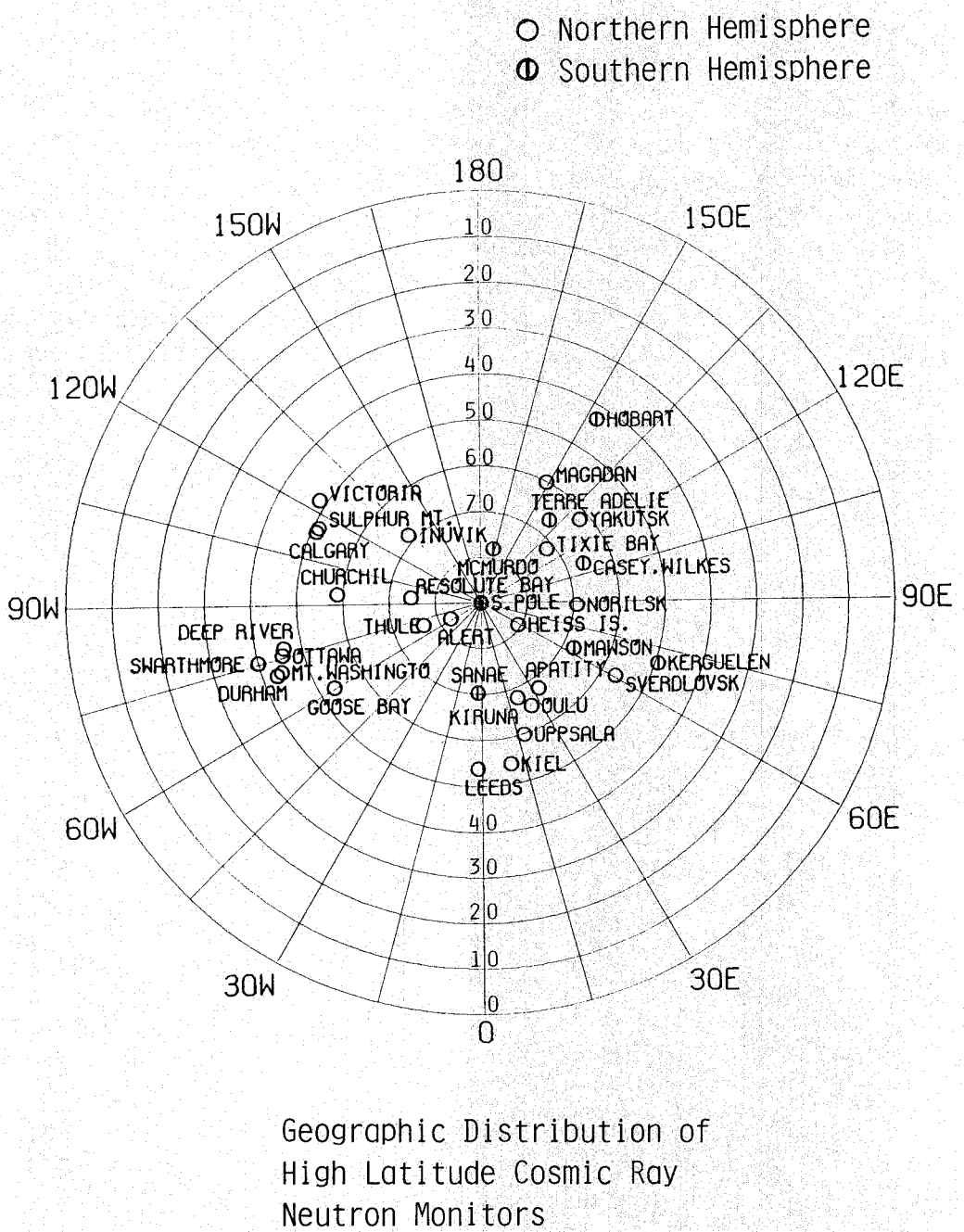

Geographic Distribution of
High Latitude Cosmic Ray
Neutron Monitors

Fig.7. Geographic distribution of high latitude neutron monitors used in the spherical harmonic analysis.

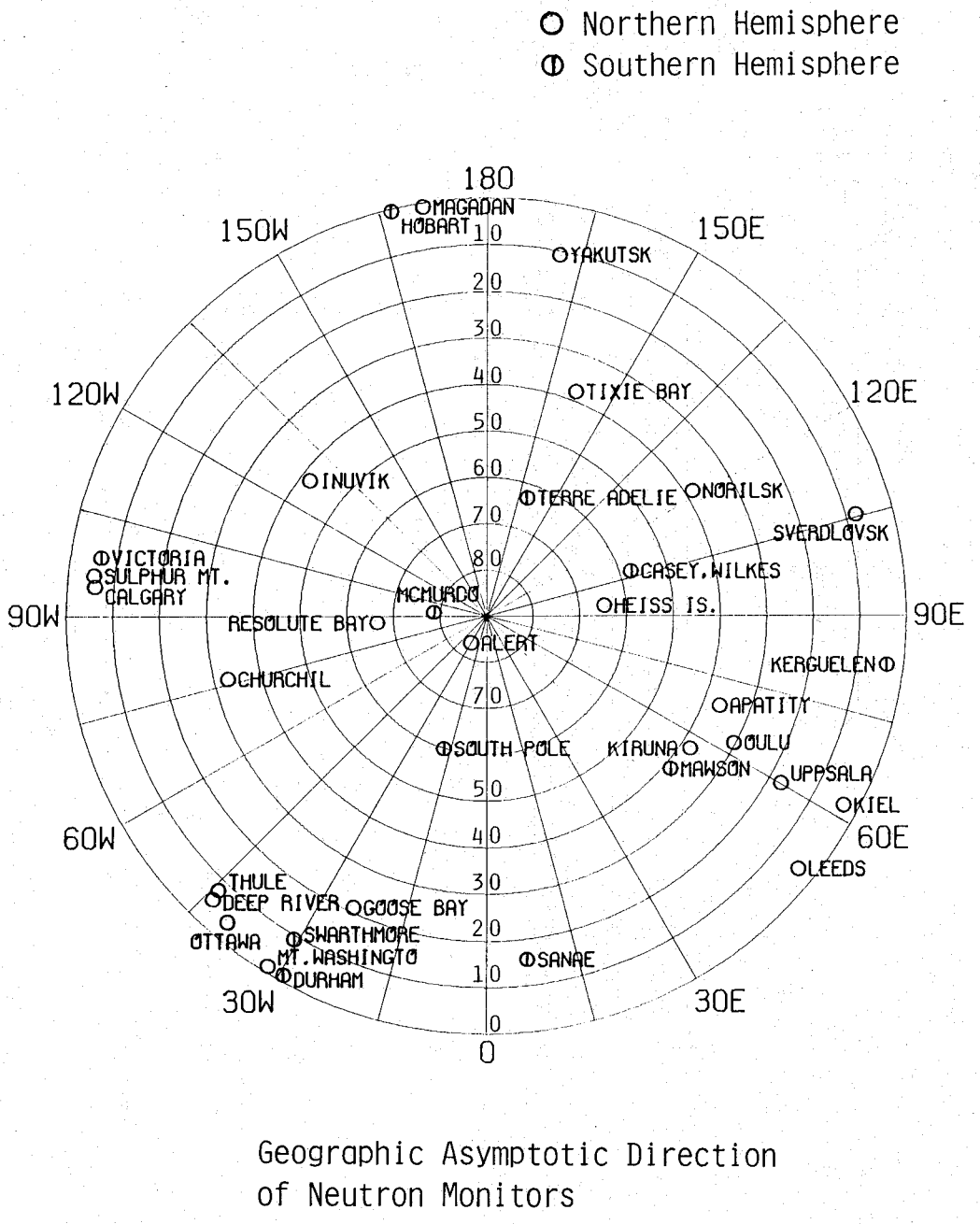

Geographic Asymptotic Direction
of Neutron Monitors

Fig.8. Geographic distribution of the asymptotic directions (for rigidity 9.5 GV) of high latitude neutron monitors used in the spherical harmonic analysis.

Table 3. List of the high latitude cosmic ray neutron monitors.

NO.	STATION	HEIGHT	VERTICAL CUTOFF RIGIDITY	ASYMPTOTIC DIRECTION 9.5 GV VERTICAL				
		(m)	(GV)	LAT.	LONG.	1966	1967	1968
1	ALERT(S)	57	0.0	83.3	−29.8	7.42	7.10	6.79
2	APATITY(S)	177	0.65	36.4	68.7	−	−	1.97
3	CALGARY(S)	1128	1.09	6.0	−94.4	11.06	11.10	10.70
4	CASEY	SL	0.01	−57.6	107.5	−	−	−
5	CHURCHIL(S)	39	0.21	33.0	−76.2	7.64	7.37	7012
6	DEEP RIVER(S)	145	1.02	5.4	−43.8	20.67	19.98	19.37
7	DURHAM(S)	SL	1.41	−1.4	−29.4	5.93	5.68	4.07
8	GOOSE BAY(S)	46	0.52	21.1	−24.4	7.08	6.79	6.54
9	HEISS IS.	20	0.10	64.6	95.3	0.22	0.21	−
10	HOBART	SL	1.89	−0.5	−166.7	0.59	0.29	0.28
11	INUVIK(S)	21	0.18	42.1	−127.8	6.96	6.68	6.45
12	KERGUELEN(S)	SL	1.19	−3.5	82.9	7.88	7.60	7.35
13	KIEL(S)	54	2.29	3.1	61.9	6.29	6.09	5.92
14	KIRUNA(S)	400	0.54	37.8	56.7	−	−	−
15	LEEDS(S)	72	2.20	3.7	50.8	7.38	7.13	6.91
16	MAGADAN(S)	SL	2.10	0.8	−171.7	−	−	−
17	NAWSON	SL	0.22	−38.5	50.0	0.38	0.37	0.36
18	MCMURDO(S)	48	0.01	−78.7	−94.7	9.43	9.13	8.83
19	MT.WASHINGTON*	1909	1.24	1.4	−31.9	1.51	1.46	1.40
20	NORILSK(S)	SL	0.63	38.3	121.5	−	−	−
21	OTTAWA	57	1.08	3.9	−40.1	1.88	1.82	1.76
22	OULU(S)	SL	0.81	30.3	62.6	3.78	3.63	3.52
23	RESOUTE BAY(S)	17	0.0	66.6	−86.8	2.22	2.18	2.12
24	SANAE(S)	53	1.02	−15.6	6.8	1.45	1.39	1.33
25	SOUTH POLE	2820	0.11	−60.0	−17.7	2.30	2.20	2.15
26	SULPHUR MT.(S)*	2283	1.14	5.6	−96.1	8.70	8.32	7.98
27	SVERDLOVSK(S)	300	2.30	7.8	105.5	−	−	−
28	SWARTHMORE(S)	80	1.92	−9.3	−30.7	3.48	3.37	3.27
29	TERRE ADELIE(S)	45	0.01	−62.9	161.1	−	−	3.95
30	THULE(S)	260	0.0	7.7	−44.2	4.51	4.34	4.22
31	TIXIE BAY(S)	SL	0.53	37.8	158.4	7.66	7.56	7.23
32	UPPSALA	SL	1.34	17.2	60.2	0.58	0.58	0.56
33	VICTORIA(S)	71	1.86	−6.6	−98.9	4.66	4.44	4.86
34	WILKES	SL	0.01	−57.6	107.5	0.43	0.41	0.40
35	YAKUTSK	105	1.70	10.6	168.6	0.18	0.18	0.17
	YAKUTSK(S)	105	1.70	10.6	168.6	−	−	−
NUMBER OF STATIONS USED IN THE SPHERICAL HARMONIC ANALYSIS					(MAXIMUM−MINIMUM)	24−23	25−21	26−22

(S) : NM−64 MONITOR, OTHERS : IGY TYPE MONITOR

(*) : NOT USED IN THE SPHERICAL HARMONIC ANALYSIS

COUNTING RATES

(10^5/h)

1969	1970	1971	1972	1973	1974	1975	1976	1977
6.68	6.68	7.15	7.46	7.43	7.33	7.49	7.52	7.48
3.87	—	4.65	4.72	4.73	4.64	4.77	4.77	4.75
10.48	10.57	11.22	11.71	—	—	—	—	—
0.39	0.40	—	—	—	—	—	—	—
7.01	7.05	7.53	7.66	7.50	—	—	—	—
19.05	19.18	20.51	20.86	20.90	20.55	31.07	21.21	21.13
3.53	3.54	4.84	5.83	5.84	5.77	5.87	5.70	5.86
6.43	6.46	6.87	6.98	6.98	6.88	7.01	7.04	7.00
—	—	—	—	—	—	—	—	—
0.27	0.28	0.29	0.30	0.29	—	—	—	—
6.35	6.39	6.80	6.90	6.91	6.81	6.96	6.98	6.94
7.19	7.26	7.76	7.90	7.88	7.79	7.96	7.99	7.98
5.83	5.86	6.23	6.31	6.29	6.20	6.32	6.35	6.34
—	6.52	6.96	7.09	7.11	6.99	—	—	—
6.64	6.27	6.23	6.31	6.29	6.20	6.32	6.35	6.34
—	—	4.92	5.00	4.99	4.97	5.06	5.10	5.03
0.35	0.35	0.38	—	—	—	—	—	—
8.75	8.79	9.43	9.61	9.56	9.46	9.69	9.74	9.73
—	1.36	1.443	1.46	1.45	1.42	1.46	1.48	1.50
—	—	3.50	3.33	3.34	3.30	3.36	3.37	3.36
1.73	1.76	1.92	1.95	—	—	—	—	—
3.47	3.49	3.75	3.79	3.82	3.77	3.85	3.88	3.86
2.12	2.12	—	—	—	—	—	—	—
1.32	1.33	1.42	1.43	1.48	1.46	1.46	1.47	1.47
2.09	2.09	2.23	2.25	2.25	2.19	—	—	1.17
7.79	7.85	8.43	8.80	—	—	—	—	—
—	—	—	—	5.81	5.61	5.78	5.81	5.79
3.20	3.23	3.44	3.49	3.48	3.45	3.52	3.54	3.53
3.84	3.88	4.09	4.22	4.21	4.15	4.26	4.29	—
4.16	4.19	4.47	4.56	4.55	4.46	4.56	4.56	—
6.59	6.55	6.76	6.33	6.87	2.19	2.26	4.00	3.09
0.55	0.56	0.58	—	—	—	—	—	—
6.23	—	—	—	—	—	—	—	—
0.39	—	—	—	—	—	—	—	—
0.18	—	—	—	—	—	—	—	—
—	—	1.48	1.50	1.49	1.46	1.46	1.46	1.46
25−20	24−22	25−21	24−21	24−21	22−20	20−20	20−18	19−18

4. Atmospheric Effects on the Neutron Monitors

The counting rate of a neutron monitor is subjected to the integrated effect of the density variations in the atmosphere above the monitor. The variation in the counting rates due to the atmospheric origin is called "atmospheric effect". The principal parts of the atmospheric effects on the variations of the counting rates observed on the ground consist of the barometer effect and the temperature effect.

4.1. Barometer effect

The barometer effect is associated with changes in the mass of air above the monitor. The close correlation between the cosmic ray intensity and the atmospheric pressure was discovered by Myssowsky and Tuwim (1926). The barometric pressure recorded at a station is taken as a measure of this mass and therefore the correction factor, known as the attenuation and/or barometer coefficient β, is given by the following equation:

$$dN = \beta N dp$$

where dN is the change in the counting rate N due to a change dp in the atmospheric pressure p.

4.2. Temperature effect

The counting rate $N_i(R_c, p, t)$ of a cosmic ray neutron monitor at a time t, is usually written for the secondary component i in the following integral representation:

$$N_i(R_c, p, t) = \int_{R_c}^{\infty} Y_i(R, p)\, j(R, t)\, dR$$

where R_c and p are the cutoff rigidity and atmospheric depth (pressure), respectively. The quantity $Y_i(R, p)$ is the gross specific yield function of the secondary component i generated from the primary particles with rigidity R, and the quantity $j(R, t)$ is the primary differential rigidity spectrum at a time t.

The atmospheric parameter appearing explicitly in eq.(4.2) is the atmospheric depth. The correction for the atmospheric effects is to transform N_i observed at an atmospheric depth to a value at a selected standard depth. This transformation is possible as far as the cascade process producing the component i involves only particles whose life time is enough long in comparing with the time of flight from their point of generation.

This situation is not always fulfilled for any component. For example, the relativistic life time of a 3 GV muon is roughly equal to the time of flight from the 100 mb level to sea level. The muon intensity at sea level is therefore strongly dependent on the density and temperature distribution throughout the atmosphere. In the case of the low energy nucleon component, a significant dependence on the atmospheric temperature arises only through a pion link in the nucleon cascade. Owing to the short life time of the pion this contribution is too small to be a somewhat significant temperature effect. The order of magnitude will be roughly estimated in the followings (Bercovitch, 1967).

The median energy of the primaries detected by sea level high latitude neutron monitors is about 20 GV. We note that this energy is divided roughly equally at the first interaction in the atmosphere (at a mean depth of ~ 60 g/cm^2) between fast nucleons and two or more charged pions with average energies of less than 5 GV.

If Γ_D is the probability of pion decay per unit time and the Γ_I the probability of nuclear interaction, then

$$\Gamma_D = \frac{1}{\Gamma_\pi \gamma_\pi}, \qquad \Gamma_I = \frac{c\rho}{\lambda_\pi}, \tag{4.3}$$

where Γ_π is the pion energy in units of rest mass, τ_π is the pion lifetime of 2.5×10^{-8} sec, ρ is the atmospheric density at a depth of 60 g/cm^2 and λ_π is the interaction mean free path. Thus, it follows that

$$\frac{\Gamma_I}{\Gamma_D} = \frac{c\rho\gamma_\pi\tau_\pi}{\lambda_\pi} \sim 12.5\,\gamma_\pi\rho, \tag{4.4}$$

for $\rho \sim 10^{-4}$ gm/cm^3 and $\gamma_\pi = 35(\sim 5$ GeV), $\Gamma_I/\Gamma_D \sim 0.045$. This means that about 4 % or less of the energy of the nucleonic cascade is transmitted through a pion link at the first interaction. Since ρ changes by about -0.5% per 1℃, the effect of the temperature change on the fluxes of the nucleonic component near the top of the atmosphere is of the order of -0.02%/℃ or less. In typical cases such an order of the temperature effect can be neglected.

Although the nucleon component has little atmospheric temperature effect, an appreciable contribution of muons to the counting rate of a sea level neutron monitor introduces a significant temperature dependence. Since the muons involved there are found near the termination of their flight range, their negative temperature effect is considerably larger than for the muon flux alone. As a result the neutron temperature effect becomes large. Dorman (1958) has calculated the temperature coefficients to apply to the correction of neutron monitor data.

Kaminer *et al.* (1965) have investigated the annual temperature effect by comparing neutron counting rates at a station in the Northern Hemisphere with that at the geomagnetically corresponding station in the Southern Hemisphere. They find an annually seasonal wave of 1.2% in amplitude from comparative studies between the Hobart and Chicago neutron data, being about 1.8 times the value theoretically obtained by using Dorman's temperature coefficients. Thus the atmospheric temperature effect on neutron is found as small as one fifth of that of muons.

4.3. Equation for the barometer coefficient

Let us consider how the mass absorption coefficient of neutrons depends on the atmospheric depth, the cutoff rigidity and the primary spectrum. The subscript i in eq.(4.2) will be from now on omitted for treating mainly neutron components.

We define the barometer coefficient in eq.(4.1) as follows:

$$\beta(R_c, p, t) = \frac{1}{N(R_c, p, t)} \frac{\partial N(R_c, p, t)}{\partial p}$$

$$= \frac{1}{N} \int_{R_c}^{\infty} \frac{\partial Y(R, p)}{\partial p} j(R, t) dR \tag{4.5}$$

$$= \frac{1}{N} \int_{R_c}^{\infty} \beta'(R, p) \frac{\partial N}{\partial R} dR \tag{4.6}$$

where

$$\beta'(R, p) = \frac{1}{Y(R, p)} \frac{\partial Y}{\partial p}. \tag{4.7}$$

The expression $\beta'(R, p)$ is the differential absorption coefficient for particles that arise from the primaries with a specific rigidity R. It should be noted that β' does not depend on the primary spectrum $j(R, t)$ whereas β depends on it.

It is evident from eq. (4.5) that the barometer coefficient β depends upon the shape of the primary spectrum. In general, any modulation of $j(R, t)$ varies in greater extent at lower rigidities than at higher rigidities, and also the coefficient β tends to decrease as the intensity decreases, since the coefficient β' increases with decreasing energy.

The spectrum dependent changes of β were first pointed out by McCracken and Johns (1959). They noted that 2% decrease in β at high latitudes was introduced when a large Forbush decrease of 10% in amplitude occurred.

4.4. Influence of the high winds

In applying corrections for the barometric effect to the secondary component measured a possible difference between the air mass above the apparatus and the reading of the barometer when strong wind blow should be noted. This difference, arising from the so-called Bernoulli's effect, is proportional to the square of the wind velocity. In a practice, the influence of the wind to the neutron component is dominant when the wind velocity is beyond 10 m/s.

At Syowa Station (69.00°S, 39.59°E, cutoff rigidity: 0.39 GV, sea-level), Antarctica, continuous observations of cosmic ray neutron intensity have been made using the 12-NM64 neutron monitor since February 1969. Using the data obtained during two years up to March 1971, possible deviation of the observed barometric pressures due to high winds were investigated in typical 8 examples of high winds over 30 m/s as shown in Fig. 9.

It is shown that the pressure deviation inferred from cosmic ray data is appreciably reduced by use of a specially designed barometric sensor (Shimizu *et al.*, 1967), but it amounts to about 4 mb in maximum when the wind velocity exceeds 30 m/s. This deviation is still higher by one order as compared with a value of 0.2 mb obtained from the wind tunnel experiment that had been carried out under the same wind condition. Figure 10 shows an example of the effect of strong wind on the neutron intensity correction for atmospheric pressure observed by using the specially designed barometric sensor at Syowa Station.

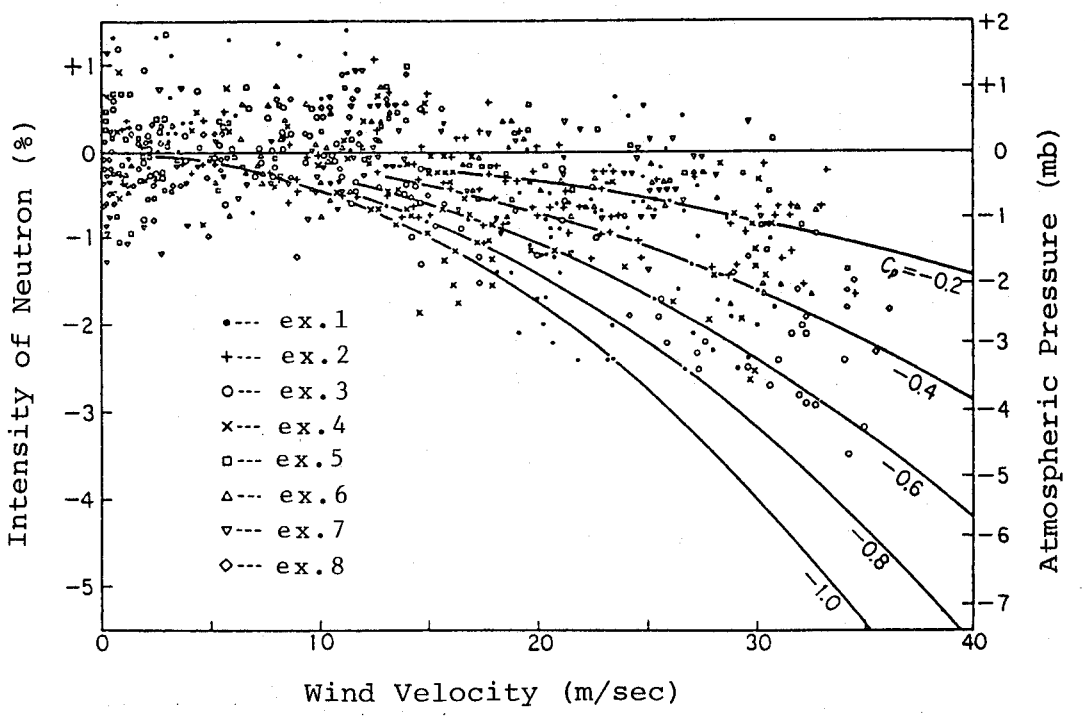

Fig.9. The relation between the neutron monitor intensity deviation and the atmospheric pressure deviation caused by high wind observed at Syowa station, Antarctica. (Kusunose and Kodama, 1972)

As has been reported by Kawasaki (1966, 1972), there are two problems in neutron observation at Mt. Norikura (36.11°N, 137.55°E, cutoff rigidity: 11.4 GV, altitude: 2770 m):

(1) Barometer coefficient of Mt. Norikura neutron monitor is 0.64 %/mb (=0.85 %/mmHg), which is extraordinary lower than that expected from the values obtained at other stations, and

(2) the time variations of the barometer corrected intensity frequently suggest abnormal pattern compared with the data of other stations, specially with those at Tokyo that should show almost the same variations.

The barometer readings at the mountain observatory that are affected by high winds through the dynamic pressure effect are corrected reasonably by the free air pressures that are estimated from the interpolations of radiosonde data of corresponding altitude (Kawasaki, 1979; Kawasaki *et al.*, 1983; Kawasaki and Wada, 1983).

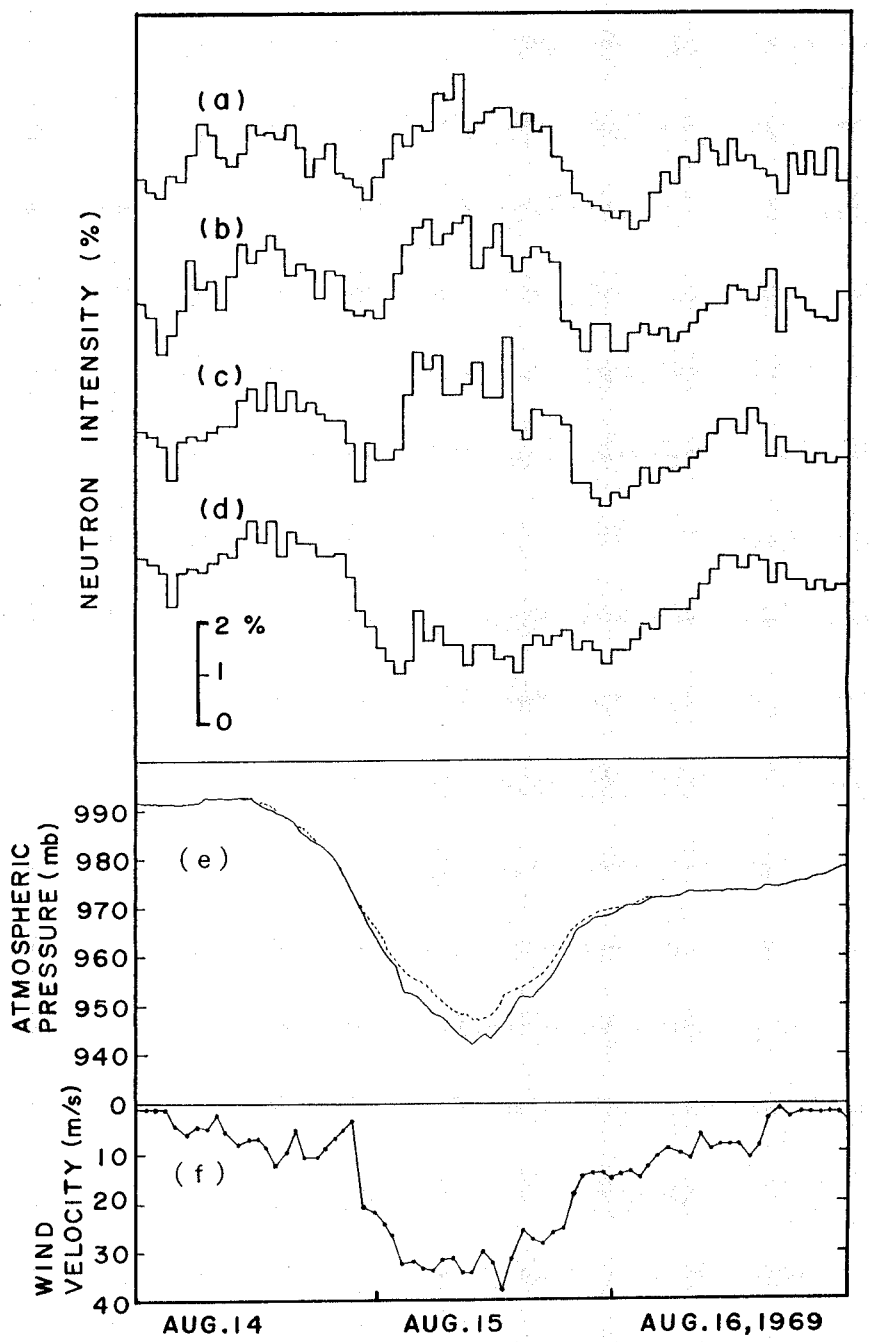

Fig.10. An example of the effect of strong wind on the neutron intensity correction for atmospheric pressure observed at Syowa Station. (a) Apatity. (b) Oulu. (c) Syowa Neutron intensity corrected for the wind velocity corrected atmospheric pressure. (d) Syowa Neutron intensity corrected for the wind velocity uncorrected atmospheric pressure. (e) Syowa atmospheric pressure. Dotted line means correction for wind velocity. (f) Syowa wind velocity. (Kusunose and Kodama, 1972)

5. Examination of the Barometer Coefficients

As described in the previous section, the barometric correction of the observed counting rates of ground based neutron monitor is important and unavoidable process. The purpose of the present section is to examine the barometer coefficients of high latitude neutron monitors that are used for barometric correction of data. Barometer coefficients that are used for the barometric correction are usually determined by individual observatories. It is not easy to examine the value of the barometer coefficient in use at each station. At a single station, the successive differencing method (Lapointe and Rose, 1962) and the autoregressive method (Martinelle, 1968) have been proposed. However, it is not proper to examine the barometer coefficient in the earth's scale. Through the study of the correlations between the daily mean pressures and the residuals of the observed data from which the composed intensities were removed, re-evaluation of the barometer coefficients have been performed. (Ogita *et al.*, 1973; Kusunose *et al.*, 1981; Kusunose, 1984)

In eq. (4.1), the barometer coefficient β is determined statistically from the linear regression analysis between the neutron intensity and the barometric pressure. Our first objective is to examine whether the barometer coefficients used in the existing cosmic ray stations are appropriate or not. We evaluate how large in the order of magnitude is the residual variation that is a possible pressure-dependent term still remained in the pressure corrected neutron intensity data supposedly caused by improper coefficients. The observed counting rates of incident particles depend upon the characteristics inherent to the observational apparatus and environment.

Therefore, the counted number of particles coming from the apparatus aiming direction must be transformed into that for unit area, unit solid angle and unit time. However, in studying the time variations of cosmic ray intensity, use of the relative intensity is convenient. Using the relative intensity, one can disregard the differences due to the size of apparatus. The pressure corrected neutron intensity N_{cor} is transformed into percentage values I_{cor} relative to the mean value. After this we use the relative percentage values in place of counting rates.

To eliminate the longitudinal component, the daily mean values are used. We define the composite neutron intensity to be

$$\overline{Y}(\phi)=C_0+C_1\sin\phi \tag{5.1}$$

where $\phi=\pi/2-\theta$ is the geographic asymptotic latitude. The harmonic coefficient C_0 and C_1 were obtained in Section 3. The function $\overline{Y}(\phi)$ is the composite neutron intensity for the cosmic ray station at asymptotic latitude ϕ.

The composite intensity $\overline{Y}$ is derived from the analysis by using data from nearly twenty stations, so the effect of improper barometer correction at some stations is reduced to about a tenth of the pressure corrected neutron intensity variation at each station. The difference ΔI between I_{cor} and $\overline{Y}(\phi)$ for a neutron monitor located at an asymptotic latitude ϕ, that is,

$$\Delta I = I_{cor} - \bar{Y}(\phi), \tag{5.2}$$

minimizes the effect of the intensity variations of the primary cosmic rays outside the magnetosphere. In this way, the remaining small pressure effect that may be included in the pressure corrected data becomes apparent by inspection of plots on the diagram of δI against the barometric pressure.

The residual barometer coefficient $\Delta\beta$ is obtained as a linear regression coefficient from the correlation between the atmospheric pressure p and the residual intensity variation ΔI defined by eq. (5.2). Thus derived values of $\Delta\beta$ for the period from 1966 to 1977 are presented in Table 5.1. The errors of coefficients in Table 5.1 stand for the standard errors of the linear regression coefficients derived from this analysis. The barometer coefficients β reported at each station are also given.

Figure 11(a) and (b) are examples of the correlation between the pressure corrected neutron intensity I_{cor} and the barometric pressure p, at (a) Deep River, 1968 and (b) Kerguelen, 1968. There appears no indicative of any correlation bewtween I_{cor} and p as seen in two figures. Figure 12(a) and (b) show the correlation between the residual neutron intensity ΔI and the barometric pressure p, at (a) Deep River, 1968 and (b) Kerguelen, 1968. There is no correlation between ΔI and p in Fig. 12(a), but the correlation is seen clearly in Fig. 12(b). It seems necessary that the barometer coefficient at Kerguelen Station in 1968 should be re-corrected.

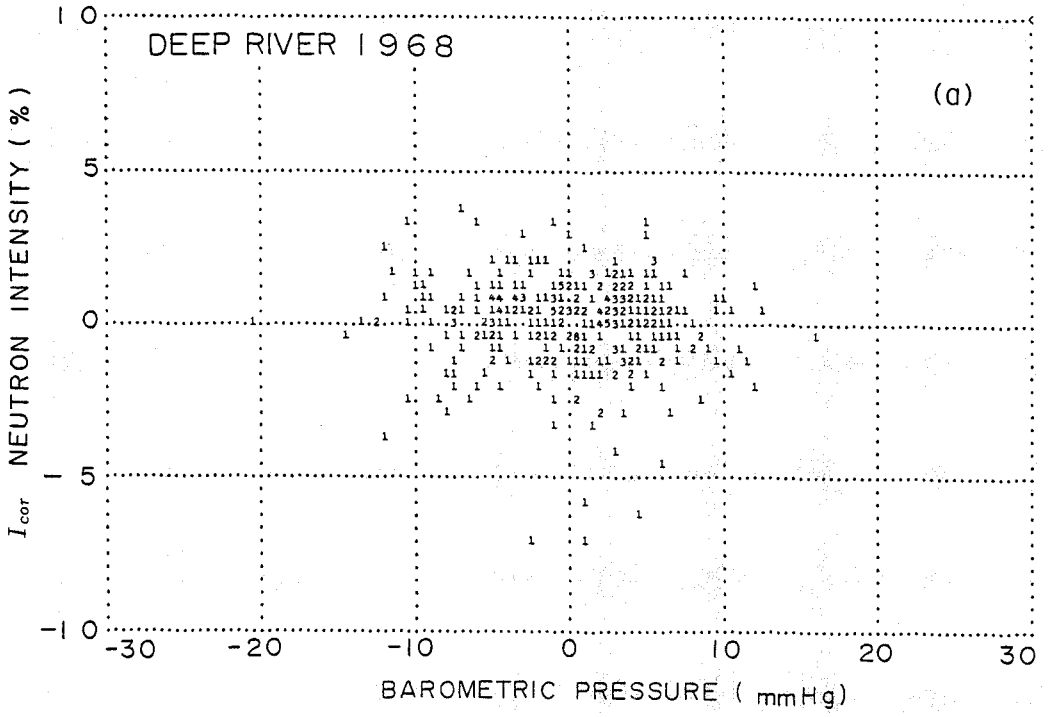

Fig.11. The relation between the cosmic ray neutron monitor intensity and barometric pressure. (a) Deep River, 1968

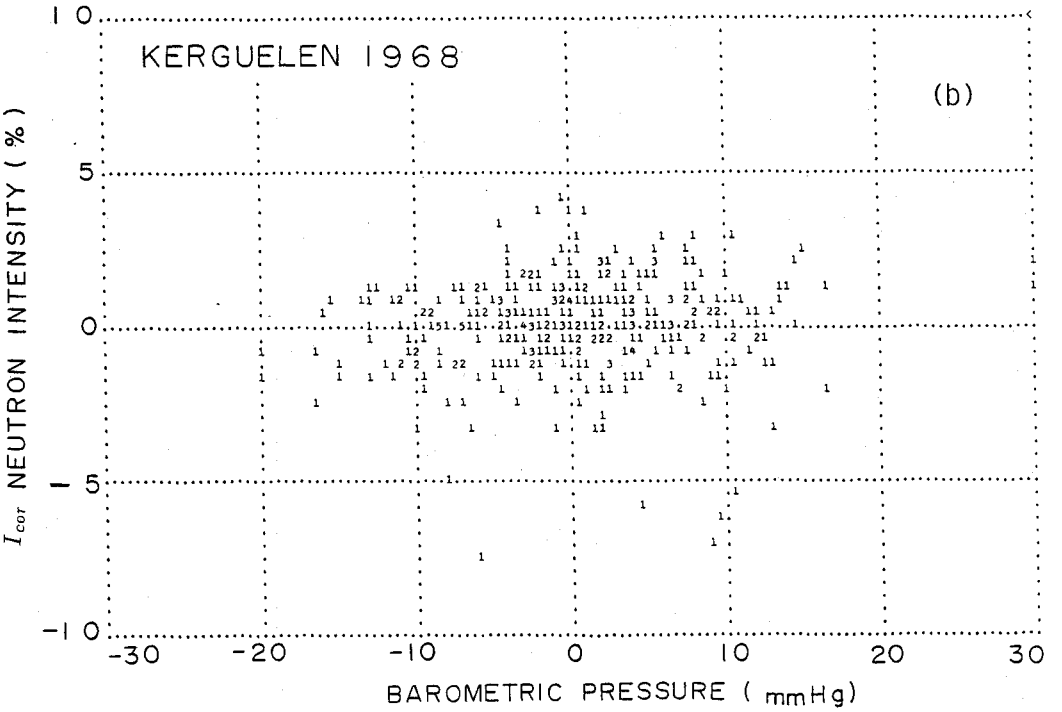

Fig.11. The relation between the cosmic ray neutron monitor intensity and barometric pressure. (b) Kerguelen, 1968

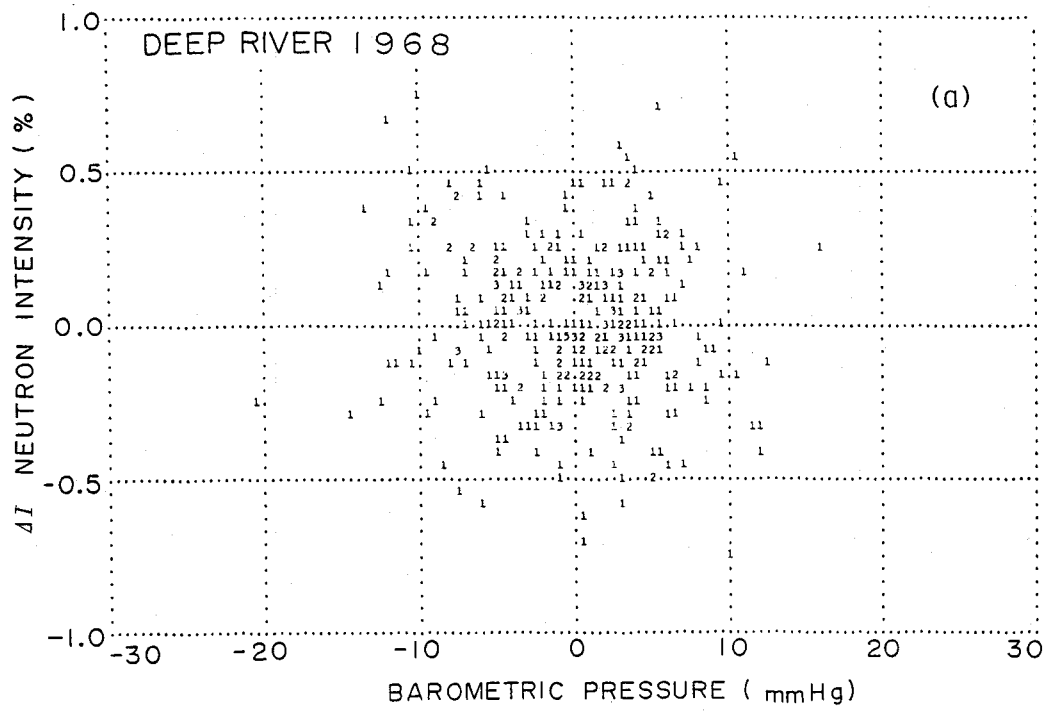

Fig.12. The relation between the residual ΔI of cosmic ray neutron intensity and the barometric pressure p. (a) Deep River, 1968

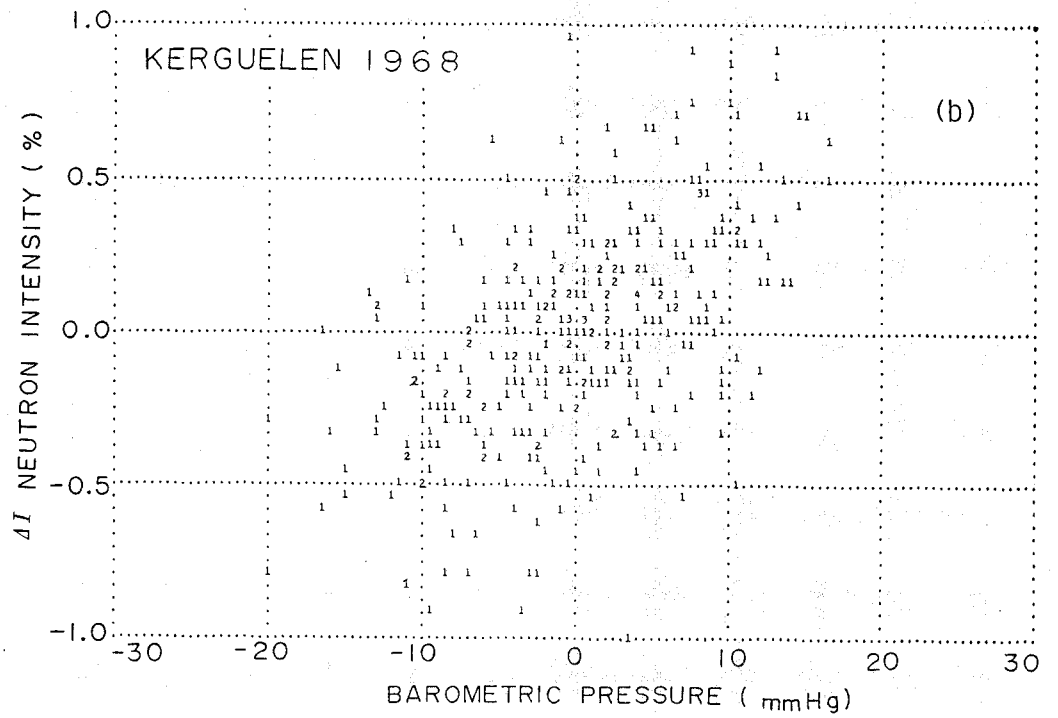

Fig.12. The relation between the residual ΔI of cosmic ray neutron intensity and the barometric pressure p. (b) Kerguelen, 1968

Figure 13 (a) shows the relation between the reported barometer coefficient β and the used standard pressure p_0. As seen in the figure the reported barometer coefficients of individual stations scatter widely even at an identical standard pressure. Two curves are observed barometer coefficients (%/mmHg) of the nucleonic component as a function of atmospheric depth (mmHg), for stations at cutoff rigidity of 2 GV.

Those curves are obtained by the different two works (BA: Bachelet *et al.*, 1965, CB: Carmichael and Bercovitch, 1969). From the reported barometer coefficient β and the residual barometer coefficient $\Delta\beta$, the corrected pressure coefficients

$$\beta_{cor} = \beta + \Delta\beta. \tag{5.3}$$

The dependence of the corrected pressure coefficients β_{cor} on the pressure is presented in Fig. 13 (b). Scattering of the points in (b) is much smaller than in (a). This suggests that the newly derived values of β_{cor} are evaluated to be more accurate than β.

Table 4 is the list of cosmic ray stations from which neutron data are used in the present analysis. Two stations, Mt. Washington and Sulphur Mt. are excluded from the spherical harmonic analysis because they are mountain stations, but are applied to the examination of barometer coefficients.

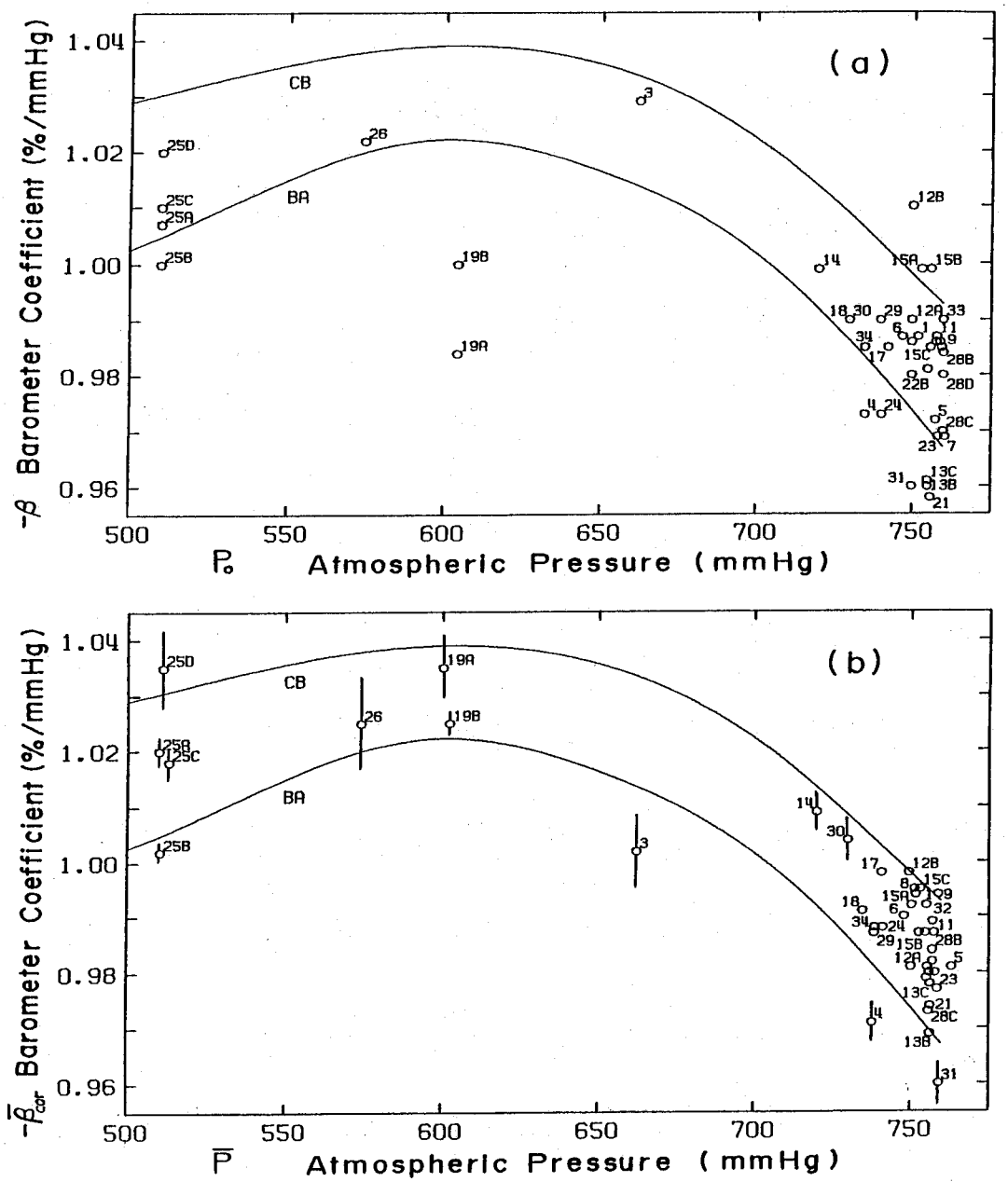

Fig.13. Barometer coefficient and atmospheric pressure. Figures attached to marks correspond to those in Table 5.1. Curves are reproduced from the papers, BA: 1962-1963, Bachelet *et al.* (1965). CB: 1965, Carmihael and Bercovitch (1969).

(a) β:the barometer coefficients of the neutron monitors and p: the standard atmospheric pressure, those are reported from respective stations.

(b) $\bar{\beta}_{cor}$:the mean barometer coefficients corrected by the present analysis. Error bars mean the standard deviations. $\bar{p}$:mean pressure. The period of averages correspond to their respective analyzed years as given in Table 5.1.

Table 4. List of the residual barometer coefficients. (Kusunose, 1984)

NO.	STATION	Po (mmHg)	$\bar{P}$ (mmHg)	β (%/mmHg)	1966	1967	1968
1	ALERT(S)	752.0	751.8	−0.987	−.008±2	−.010±2	.004±3
2	APATITY(S)	750.0	742.1	−0.906	−	−	−.024±6
3	CALGARY(S)	662.3	662.4	−1.029	.017±3	−.020±3	.035±3
4	CASEY	735.0	737.9	−0.973	−	−	−
5	CHURCHIL(S)	757.5	763.3	−0.972	−.013±2	−.008±2	−.001±2
6	DEEP RIVER(S)	747.0	748.0	−0.987	−.006±2	.007±2	−.004±2
7	DURHAM(S)	760.5	* * *	−0.969	* * *	* * *	* * *
8	GOOSE BAY(S)	758.0	751.4	−0.987	−.002±2	.005±2	.002±2
9	HEISS IS.	759.0	759.0	−0.986	−.008±4	−	−
10	HOBART	759.5	754.8	−0.985	−.019±3	−.001±3	−.007±3
11	INUVIK(S)	758.0	757.6	−0.987	−.001±2	.004±2	.012±2
12	KERGUELEN(S) A	750.0	750.2	−0.99	.009±3	−	−
	KERGUELEN(S) B	750.0	749.6	−1.01	.007±2	.018±2	.026±2
13	KIEL(S) A	755.0	755.2	−0.981	−.003±2	.004±2	.008±2
	KIEL(S) B	755.0	756.3	−0.969	−	−	.000±3
	KIEL(S) C	755.0	756.1	−0.961	−	−	−
14	KIRUNA(S)	720.0	720.2	−0.999	−	−	−
15	LEEDS(S) A	753.0	750.4	−0.999	.005±2	.004±1	.007±2
	LEEDS(S) B	756.0	752.8	−0.999	−	−	−
	LEEDS(S) C	756.0	753.3	−0.985	−	−	−
16	MAGADAN(S)	736.8	* * *	−0.946	−	−	−
17	NAWSON	742.5	740.9	−0.985	−.007±3	−.007±3	.001±2
18	MCMURDO(S)	730.0	734.7	−0.99	−.006±1	−.006±2	−.002±2
19	MT.WASHINGTON A	604.5	600.3	−0.984	−.052±6	−	−
	MT.WASHINGTON B	604.5	602.5	−1.000	−.021±6	−.026±6	
20	NORILSK(S)	745.1		−0.920	−	−	−
21	OTTAWA	756.0	756.4	−0.958	−.022±3	−.011±3	−.025±3
22	OULU(S) A	750.0	757.2	−0.986	−.001±2	.003±2	.007±2
	OULU(S) B	750.0	757.2	−0.980	−	−	−
23	RESOUTE BAY(S)	758.3	758.8	−0.969	−.022±3	−.014±3	−.003±3
24	SANAE(S)	740.4	741.2	−0.973	−.009±3	−.002±3	−.011±3
25	SOUTH POLE A	510.0	510.0	−1.007	−.013±3	−	−
	SOUTH POLE B	510.0	510.6	−1.000	−	−.006±3	−.001±3
	SOUTH POLE C	510.0	513.2	−1.010	−	−	−
	SOUTH POLE D	510.0	511.2	−1.020	−	−	−
26	SULPHUR MT.(S)	574.5	574.3	−1.022	−.015±3	−.015±6	−.005±3
27	SVERDLOVSK(S)	* * *	* * *	−0.960	−	−	−
28	SWARTHMORE(S) A	760.0	758.0	−0.99	.010±5	−	−
	SWARTHMORE(S) B	760.0	757.1	−0.984	.000±4	−	−
	SWARTHMORE(S) C	760.0	755.9	−0.97	−	−.007±3	−.009±3
	SWARTHMORE(S) D	760.0	755.5	−0.98	−	−	−
29	TERRE ADELIE(S)	740.0	738.4	−0.99	−	−	.009±3
30	THULE(S)	730.0	730.1	−0.99	−.013±2	−.011±2	−.010±3
31	TIXIE BAY(S)	750.0	759.3	−0.960	−.024±3	−.017±2	−.023±1
32	UPPSALA	757.8	755.2	−0.986	−	* * *	* * *
33	VICTORIA(S)	760.0	756.1	−0.99	.011±3	.008±3	.018±6
34	WILKES	735.0	738.6	−0.985	−.005±3	−.003±2	.002±3
35	YAKUTSK A	750.0	752.1	−0.906	−.010±7	.019±6	−.007±8
	YAKUTSK(S) B	750.0	* * *	−0.906	−	−	−

Po : STANDARD PRESSURE, $\bar{P}$: MEAN PRESSURE
β : REPORTED BAROMETER COEFFICIENT
− : NO DATE, * * * : NOT REPORTED PRESSURE DATA

RESIDUAL BAROMETER COEFFICIENT (%/mmHg)								
1969	1970	1971	1972	1973	1974	1975	1976	1977
.000±2	−.001±3	−.009±2	−.004±2	−.007±2	−.007±2	−.012±2	−.016±1	−.012±2
.014±7	* * *	* * *	* * *	* * *	* * *	* * *	* * *	* * *
.033±3	.034±3	.025±4	.027±3	—	—	—	—	—
.006±3	−.001±2	—	—	—	—	—	—	—
−.004±2	−.005±2	−.012±2	−.018±2	−.010±2	—	—	—	—
.005±2	.007±2	−.006±2	.000±2	.007±2	−.001±2	−.004±2	−.012±2	−.013±2
* * *	* * *	* * *	* * *	* * *	* * *	* * *	* * *	* * *
.010±2	.007±2	.000±2	−.017±2	−.017±2	−.018±2	−.018±2	−.021±2	−.022±2
—	—	—	—	—	—	—	—	—
.007±3	.006±3	−.001±3	—	—	—	—	—	—
.010±2	.012±2	.006±1	−.006±2	−.006±2	−.002±2	−.012±2	−.006±2	−.012±2
—	—	—	—	—	—	—	—	—
.024±2	.025±2	.012±2	.004±2	.008±2	.005±2	.010±2	.003±2	.003±2
.002±3	—	—	—	—	—	—	—	—
—	—	—	—	—	—	—	—	—
−.002±2	−.003±2	−.013±2	−.012±2	−.023±2	−.019±2	−.024±2	−.025±2	−.022±2
—	−.015±2	−.005±2	−.008±2	−.008±1	−.013±2	—	—	—
.015±3	—	—	—	—	—	—	—	—
.013±3	.012±2	—	—	—	—	—	—	—
—	—	−.014±1	−.011±2	−.017±1	−.011±1	−.011±2	−.004±1	.000±2
—	—	* * *	—	—	—	—	—	—
−.011±3	−.017±3	−.039±4	—	—	—	—	—	—
.002±2	.005±2	−.003±2	−.003±2	−.008±2	−.004±1	.002±2	.004±2	−.012±4
—	—	—	—	—	—	—	—	—
* * *	* * *	* * *	* * *	* * *	* * *	* * *	* * *	* * *
—	—	* * *	* * *	* * *	* * *	* * *	* * *	* * *
−.015±3	−.017±3	−.034±3	−.027±4	—	—	—	—	—
.007±2	—	—	—	—	—	—	—	—
—	.001±3	.002±3	−.001±4	−.017±2	−.009±2	−.011±2	−.014±1	−.021±2
−.003±3	.004±3	—	—	—	—	—	—	—
−.003±3	−.007±3	−.013±3	−.013±3	−.015±4	−.018±2	−.028±3	−.034±3	−.021±3
—	—	—	—	—	—	—	—	—
.000±3	.002±2	—	—	—	—	—	—	—
—	—	−.008±4	—	—	—	—	—	—
—	—	−.012±4	−.023±3	−.022±3	−.005±3	—	—	—
.003±4	.006±4	−.013±4	.005±5	—	—	—	—	—
—	—	—	—	* * *	* * *	* * *	* * *	* * *
—	—	—	—	—	—	—	—	—
—	—	—	—	—	—	—	—	—
.018±3	−.007±3	−.020±3	—	—	—	—	—	—
—	—	−.005±4	−.005±2	−.004±2	−.001±3	.008±3	.000±3	.001±5
.011±2	.001±3	−.002±3	−.008±3	.014±3	−.005±3	.001±3	.006±3	—
−.017±3	−.011±3	−.013±2	−.016±2	−.022±2	−.010±2	−.017±2	−.007±2	—
−.016±2	−.011±3	* * *	* * *	* * *	* * *	* * *	* * *	* * *
—	−.005±3	−.009±3	—	—	—	—	—	—
—	—	—	—	—	—	—	—	—
−0.10±7	—	—	—	—	—	—	—	—
−.006±9	—	—	—	—	—	—	—	—
—	—	* * *	* * *	* * *	* * *	* * *	* * *	* * *

6. Solar Cycle Variation of the Barometer Coefficients

In this section, we discuss the problem of solar cycle variation in the barometer coefficients of high latitude neutron monitors. This matter is the second objective of the present research. (Kusunose and Ogita, 1985)

6.1. Year-to-year variation of the barometer coefficients)

Figure 14 shows the year-to-year variation of cosmic ray intensity $\bar{I}$ and also of barometer coefficient $\overline{\beta}$. Here, $\bar{I}$ and $\overline{\beta}$ are the averages of yearly mean data throughout eight neutron monitors (Alert, Deep River, Goose Bay, Inuvik, Kerguelen, Kiel, Oulu and Sanae) where the complete data without observation failure are available through 12 years from 1966 to 1977. The intensity $\bar{I}$ is normalized to 100 percent in 1966.

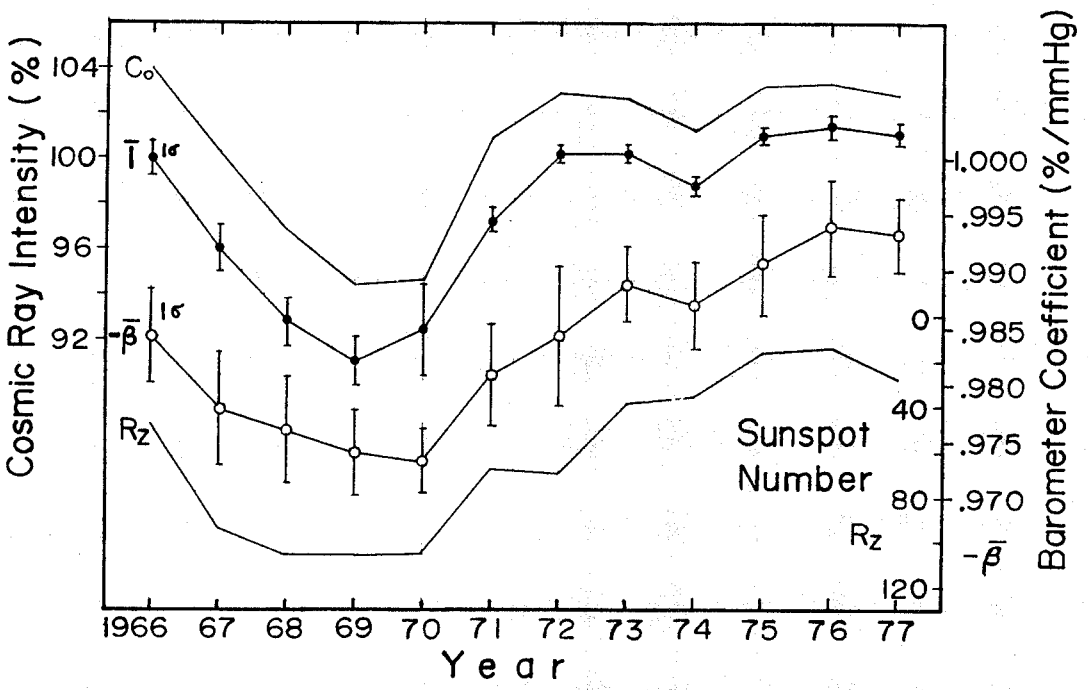

Fig.14. The year-to-year variation of C_0: the isotropic component of the spherical harmonic coefficients, $\bar{I}$: cosmic ray neutron intensity and $\overline{\beta}$: barometer coefficient, they all are the averages of eight stations and error bars show the scatter of individual station, and Rz: the sunspot number.

In Fig. 14, C_0 is the isotropic component of spherical harmonic coefficients and normalized to the value of 1966 with the whole shift toward higher level by 4%. The symbol Rz is the Zürich sunspot number inversely plotted that is an index of solar activity. The correlation between the barometer coefficient $\overline{\beta}$ and the sunspot number Rz is clearly seen in Fig. 15. Its correlation coefficient becomes 0.97.

6.2. Barometer coefficient and cosmic ray intensity

In order to investigate a possible solar modulation of the barometer coefficient, we analyze the relation between the barometer coefficient and the cosmic ray intensity. Let us define the term $\delta\beta$, to represent the solar modulation of the barometer coefficient, as

$$\beta(R_C,\ p,\ t)=\beta_0(R_C,\ p)+\delta\beta(R_C,\ p,\ t). \tag{6.1}$$

From eq. (5.1), the barometer coefficient (attenuation coefficient) is expressed as

$$\beta(R_C,\ p,\ t)=\frac{1}{N(R_C,\ p,\ t)}\frac{\partial N(R_C,\ p,\ t)}{\partial p}, \tag{6.2}$$

where $N(R_C,\ p,\ t)$ is the counting rates of cosmic ray neutrons. In the same way as eq. (6.1), if δN is the solar modulation term, then we have

$$N(R_C,\ p,\ t)=N_0(R_C,\ p)+\delta N(R_C,\ p,\ t). \tag{6.3}$$

Substituting eq. (6.3) into eq. (6.2), we obtain

$$\beta=\frac{1}{N_0+\delta N}\frac{\partial}{\partial p}(N_0+\delta N)=\frac{N_0}{N_0+\delta N}\beta_0+\frac{\delta N}{N_0+\delta N}\beta_\gamma, \tag{6.4}$$

where

$$\beta_0(R_C,\ p)=\frac{1}{N_0}\frac{\partial N_0}{\partial p},\ \text{and}\quad \beta_\gamma(R_C,\ p,\ t)=\frac{1}{\delta N}\frac{\partial}{\partial p}\delta N. \tag{6.5}$$

If we put $\delta I=\delta N/N_0$, then we have at the first order approximation

$$\beta=\frac{1}{1+\delta I}\beta_0+\frac{\delta I}{1+\delta I}\beta_\gamma=(1-\delta I)\beta_0+\delta I(1-\delta I)\beta_\gamma=\beta_0+(\beta_\gamma+\beta_0)\delta I.$$

Comparing the above result with eq. (6.1), we have

$$\delta\beta=(\beta_\gamma-\beta_0)\,\delta I=\alpha_\gamma\cdot\delta I, \tag{6.6}$$

where

$$\alpha_\gamma(R_C,\ p,\ t)=\beta_\gamma(R_C,\ p,\ t)-\beta_0(R_C,\ p). \tag{6.7}$$

If α_γ equal to zero, $\delta\beta$ is independent on δI. But as seen in Fig. 14, the absolute value of the barometer coefficient varies with cosmic ray intensity level. So α_γ is not zero. Belov and Dorman (1979) had derived β_γ, but they did not mention about anything, which is equivalent to α_γ that we have introduced here. Figure 15 shows the relation between the sunspot number and the barometer coefficient.

In eq. (6.6), we can estimate α_γ from the correlation between the barometer coefficient and the cosmic ray intensity variation. For convenience, after this we deal with α_γ in the absolute value. Figure 16 shows the relation between the barometer coefficient $\overline{\beta}$ and the cosmic ray intensity $\bar{I}$. The linear regression coefficient α_γ throughout the whole period is found to be $\alpha_\gamma=(1.83\pm0.24)\ 10^{-3}/\text{mmHg}$ with the correlation coefficient of 0.92.

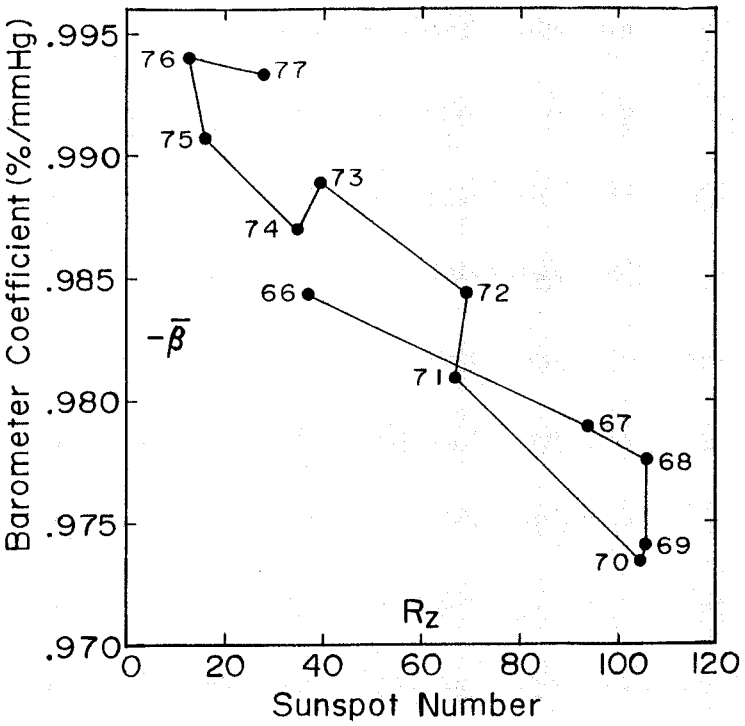

Fig.15. Relation between the barometer coefficient $\bar{\beta}$ and the sunspot number Rz from 1966 to 1977.

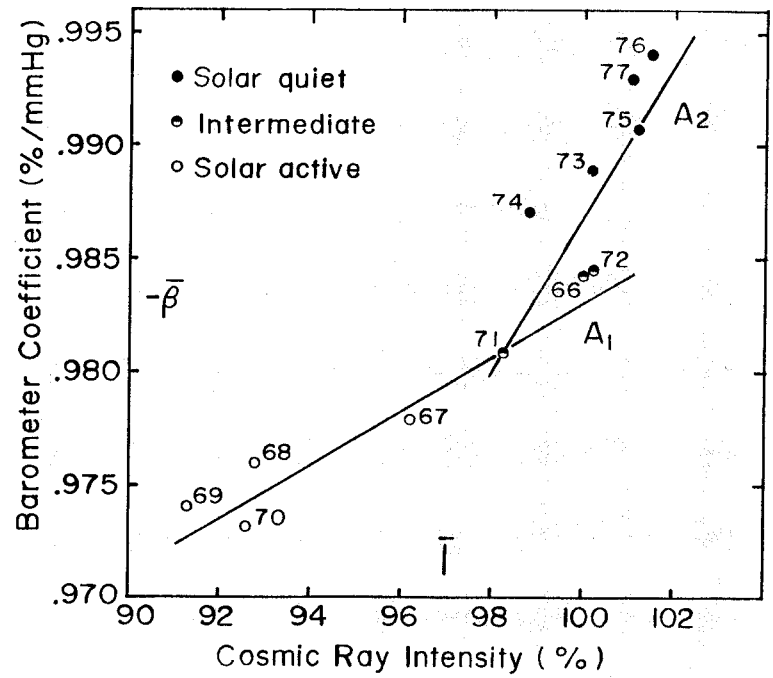

Fig.16. Relation between the barometer coefficient $-\bar{\beta}$ and cosmic ray intensity $\bar{I}$. Lines A_1 and A_2 represent the linear regression line between the barometer coefficient and the cosmic ray intensity in the solar active and the solar quiet period respectively.

We may separate the distribution of points in Fig. 16 into two parts of the solar active period, A_1 (1966 - 1972) and the solar quiet period, A_2 (1966, 1971 - 1977). Years 1966, 1971 and 1972 are included together in both parts as the intermediate period. The two regression coefficients α_γ's are calculated separately for the solar active and quiet periods. They are $\alpha_\gamma=(1.20\pm0.18)\ 10^{-3}/\mathrm{mmHg}$ (r=0.97) and $\alpha_\gamma=(3.25\pm0.69)\times10^{-3}/\mathrm{mmHg}$ (r=0.74), respectively.

Next we compare our results with those reported by other authors. The point G in Fig. 17 is estimated from the figure given by Griffiths it *et al.* (1965) being $\alpha_\gamma=(4.2\pm0.9)\times10^{-3}/\mathrm{mmHg}$ (r=0.97). The analysis was made for 12 years data over the preceding solar cycle 1954 - 1965. The value of α_γ at G is larger than our present result for the succeeding solar cycle 1966 - 1977.

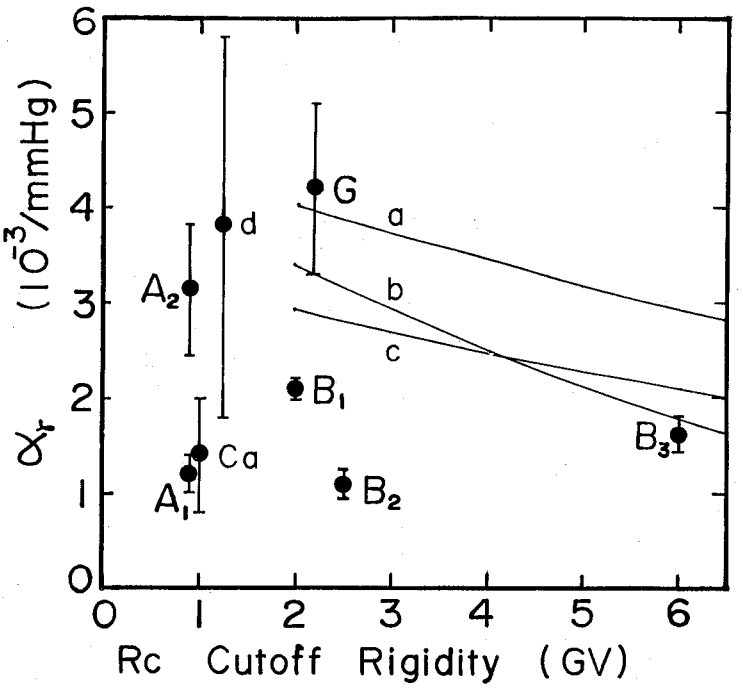

Fig.17. Distribution of α_γ, which is defined as $\alpha_\gamma=\delta\beta/\delta I$, and plotted in absolute value. The abscissa is the cutoff rigidity where the neutron monitor is located, or the mean rigidity at several stations.
A_1 ($R_c\leq2.3$ GV, altitude $\leq$ 145m, 1966-1972) and A_2 (1966, 1971-1977): The present work.
B_1 ($R_c<2.8$GV, altitude $<$ 750m, 1957-1969), B_2 ($R_c<4.5$GV, altitude $>$ 1900m, 1957-1969) and B_3 ($R_c\sim6.5$GV, altitude $\leq$ 500m, 1957-1969):Bachelet *et al.* (1972d).
Ca (Deep River, 1965-1969): Carmichael and Peterson (1971).
G (Leeds, 1954-1965): Griffiths *et al.* (1965).
a, b, c (High latitudes, normalized at a pressure of 500mmHg) and d (Sanae): Raubenheimer and Stoker (1974).

Points B_1 and B_2 are the results obtained by Bachelet *et al.* (1972). B_1, that is, $\alpha_7 = (2.12 \pm 0.08) \times 10^{-3}$/mmHg (r=0.993) is the result from high latitude stations with R_c of 2.8 GV at low altitudes ($h<750$m), while B_2 is R_c of $P \leq 4.5$GV at high altitudes ($h>1800$m). The period of analyses used for points B_1 and B_2 one solar cycle from 1957 to 1969. The value of α_7 at B_1 is consistent with our result. The value at B_2 is less than the results obtained by the airborne neutron monitors (Raubenheimer and Stoker, 1974) that are normalized to a pressure level of 500 mmHg and indicated by a, b and c in Fig. 17.

Point Ca is given by Carmichael and Peterson (1971) being $\alpha_7 = (1.4 \pm 0.6) \times 10^{-3}$/mmHg (r=0.99). The period of data analysis is 5 years from 1965 to 1969 when the solar activity was on the increasing phase from the minimum to the maximum, corresponding to A_1 period. Two points of Ca and A_1 are in good agreement with each other.

As mentioned above, the values of α_7 scatter in the range of $(1 \sim 4) \times 10^{-3}$/mmHg among high latitude stations. It also α_7 is larger in the solar quiet period than in the solar active period. From the curves a, b and c in Fig. 17, it is seen that α_7 decreases as the cutoff rigidity R_c increases. Therefore it can be interpreted that the mean rigidity of cosmic rays is smaller and α_7 is larger, when the solar activity becomes lower, compared to the higher solar activity.

7. Quantitative Relation of the Barometer Coefficient and the Cosmic Ray Primary Spectrum

In the preceding sections, it is reported that the variation rate of the barometer coefficient against the cosmic ray neutron intensity is larger in the solar quiet period than in the solar active period. The present section is concerned with the numerical calculation verifying quantatively the relation between the barometer coefficient and the cosmic ray primary spectrum variation.

7.1. Method of analysis

The counting rate of the neutron monitor at time t is expressed by

$$N(R_c,\ p,\ t) = \int_{R_c}^{\infty} Y(R,\ p)\, j(R,\ t)\, dR, \tag{7.1}$$

where R_c is the vertical cutoff rigidity, p is the atmospheric pressure or depth, $Y(R, p)$ is the yield function, and $j(R, t)$ is the rigidity spectrum of primary cosmic ray flux. Substituting eq. (7.1) into eq. (6.2), we have the barometer coefficient β in place of R_c as

$$\beta(R_c,\ p,\ t) = \frac{1}{N(R_c,\ p,\ t)} \int_{R_c}^{\infty} \frac{\partial Y(R,\ p)}{\partial p}\, j(R,\ t)\, dR, \tag{7.2}$$

From eq. (7.2) it is clear that the barometer coefficient is dependent on the primary cosmic ray spectrum.

Let the primary spectrum be

$$j(R,\ t)=j_o(R)+\delta j(R,\ t), \tag{7.3}$$

where $j_o(R)$ is the spectrum of non-modulated galactic cosmic rays near the earth and $\delta j(R,\ t)$ is for the modulated term. From eq. (7.1) and eq. (7.3), the intensity of the secondary cosmic ray at a cutoff rigidity R_c and an atmospheric depth p is

$$\begin{aligned} N(R_c,\ p,\ t)&=\int_{R_c}^{\infty} Y(R,\ p)\, j_o(R)\, dR+\int_{R_c}^{\infty} Y(R,\ p)\,\delta j(R,\ t)\, dR \\ &=N_o(R_c,\ p)+\delta N(R_c,\ p,\ t), \end{aligned} \tag{7.4}$$

where N_o and δN are defined respectively by

$$N_o(R_c,\ p)=\int_{R_c}^{\infty} Y(R,\ p)\, j_o(R)\, dR, \tag{7.5}$$

and

$$\delta N(R_c,\ p,\ t)=\int_{R_c}^{\infty} Y(R,\ p)\,\delta j(R,\ t)\, dR. \tag{7.6}$$

The barometer coefficient for the non-modulated spectrum is

$$\beta_o(R_c,\ p)=\frac{1}{N_o(R_c,\ p)}\frac{\partial}{\partial p}N_o(R_c,\ p), \tag{7.7}$$

and the coefficient for the modulated spectrum is

$$\beta_7(\mathrm{R_c,\ p,\ t})=\frac{1}{\delta N(R_c,\ p,\ t)}\frac{\partial}{\partial p}\delta\mathrm{N}(\mathrm{R_c,\ p,\ t}). \tag{7.8}$$

In eq. (7.8), it is clear that the definition of β_7 is the same as in eq. (6.5).

Relation between the coefficient β_7 and the primary variation spectrum $\delta j/j_o$ is expressed by using eq. (7.6) and eq. (7.8) as follows:

$$\beta_7(R_c,\ p,\ t)=\frac{\int_{R_c}^{\infty}\frac{\partial Y(R,\ p)}{\partial p}\delta j(R,\ t)dR}{\int_{R_c}^{\infty} Y(R,\ p)\delta j(R,\ t)dR}. \tag{7.9}$$

By using the response function $F(R,\ p)=Y(R,\ p)\, j_o(R)$, we rewrite eq. (7.9) as

$$\beta_7(R_c,\ p,\ t)=\frac{\int_{R_c}^{\infty}\frac{\partial F(R,\ p)}{\partial p}\frac{\delta j(R,\ t)}{j_o(R)}dR}{\int_{R_c}^{\infty} F(R,\ p)\frac{\delta j(R,\ t)}{j_o(R)}dR}. \tag{7.10}$$

From the definition of the response function and eq.(7.5), we have

$$N_o(R_c,\ p)=\int_{R_c}^{\infty} F(R,\ p)dR,$$

then we can write as

$$F(R,\ p)=-\frac{\partial N_o(R,\ p)}{\partial R}.$$

Differentiating by p, we have

$$\frac{\partial F(R,\ P)}{\partial p} = -\frac{\partial}{\partial R}\frac{\partial N_o(R,\ p)}{\partial p} = -\frac{\partial}{\partial R}\left[\beta_o(R,\ p)\, N_o(R,\ p)\right].$$

Substituting into eq. (7.10), we obtain

$$\beta_\gamma(R_c,\ p,\ t) = \frac{\int_{R_c}^{\infty}\frac{\partial}{\partial R}[\beta_o(R,\ p)N_o(R,\ p)]\frac{\delta j(R,\ t)}{j_o(R)}dR}{\int_{R_c}^{\infty}\frac{\partial N_o(R,\ p)}{\partial R}\frac{\delta j(R,\ t)}{j_o(R)}dR}. \tag{7.11}$$

If $\beta_o(R,\ p)$=const. with respect to R, then it follows from eq. (7.11) that $\beta_\gamma = \beta_o$. Furthermore, in this case it can be concluded from eq. (6.6) that $\alpha_\gamma = 0$. Therefore, the difference between the barometer coefficients $\beta_o(R_c, p)$ and $\beta_\gamma(R_c,\ p)$ can be attributed to the dependence of $\beta_o(R_c, p)$ on the rigidity R.

Let us assume the primary variation spectrum as

$$\delta j(R,\ t)/j_o(R) \propto R^{-\gamma}, \qquad \gamma = \gamma(t). \tag{7.12}$$

Substituting into eq.(7.11), we obtain, by partial integration,

$$\beta_\gamma(R_c,\ p,\ t) = \frac{\int_{R_c}^{\infty}\frac{\partial}{\partial R}(\beta_o N_o)R^{-\gamma}dR}{\int_{R_c}^{\infty}\frac{\partial N_o}{\partial R}R^{-\gamma}dR}$$

$$= \frac{\gamma\int_{R_c}^{\infty}\beta_o(R,\ p)N_o(R,\ p)R^{-\gamma-1}dR - \beta_o(R_c,\ p)N_o(R_c,\ p)R^{-\gamma}}{\gamma\int_{R_c}^{\infty}N_o(R,\ p)R^{-\gamma-1}dR - N_o(R_c,\ p)R^{-\gamma}}. \tag{7.13}$$

From eq. (6.7) and eq. (7.13) we can obtain

$$\alpha_\gamma(R_c,\ p,\ t) = \beta_\gamma(R_c,\ p,\ t) - \beta_o(R_c,\ p)$$

$$= \frac{\gamma\int_{R_c}^{\infty}[\beta_o(R,\ p) - \beta_o(R_c,\ p)]N_o(R_c,\ p)R^{-\gamma-1}dR}{\gamma\int_{R_c}^{\infty}N_o(R,\ p)R^{-\gamma-1}dR - N_o(R_c,\ p)R^{-\gamma}}. \tag{7.14}$$

7.2. Computation

Now let us begin to calculate the variation rate α_γ of the barometer coefficient β by using eq. (7.14). It can be computed from the rigidity dependence of the sea level barometer coefficient $\beta_o(R,\ p)$ and the cosmic ray neutron intensity $N_o(R,\ p)$.

The rigidity dependence of neutron intensity in 1965 is shown in Fig. 18, where dots represent the values given by Carmichel and Bercovitch (1969). A smoothed curve fitted to data points is used in the later computation.

Figure 19 shows the rigidity dependence of the barometer coefficient of the neutron monitor. The solid circles are the values estimated by Carmichael *et al.* (1968) from 1965 - 1966 survey data. Further extrapolation must be made for the computation of higher rigidity range. The extrapolated curve is shown in Fig. 20.

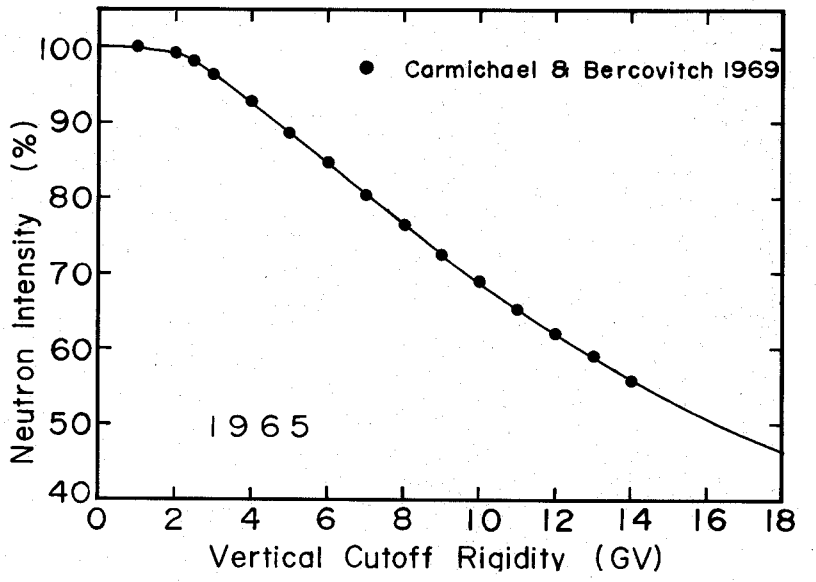

Fig.18. Rigidity dependence of cosmic ray neutron monitor intensity at sea level in 1965. The values of filled points are cited from the table given by Carmichael and Bercovitch (1969e). Curve shows the approximated value used in the numerical calculation.

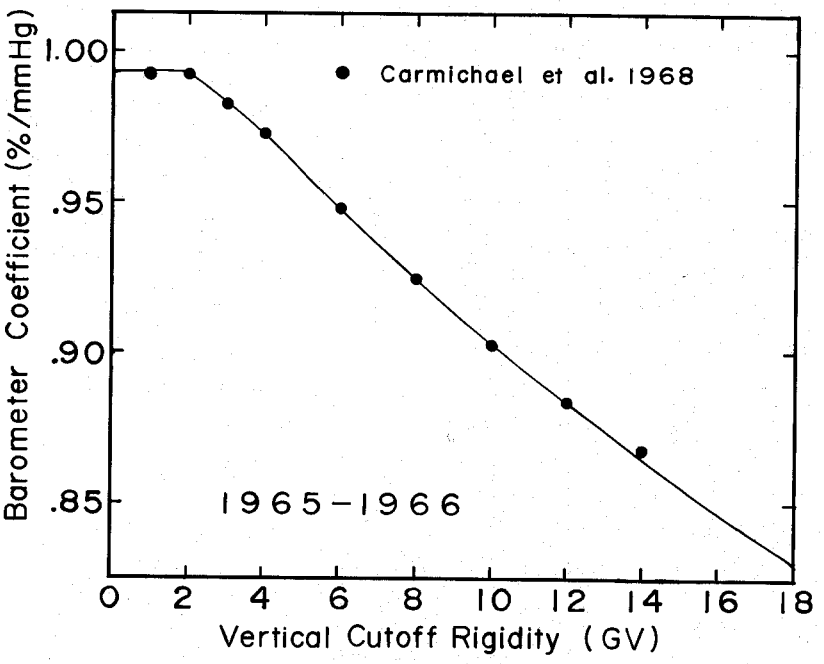

Fig.19. Rigidity dependence of neutron monitor barometer coefficient. Filled points show the values given by Carmichael *et al.* (1968). Curve shows the approximated value used in the numerical calculation.

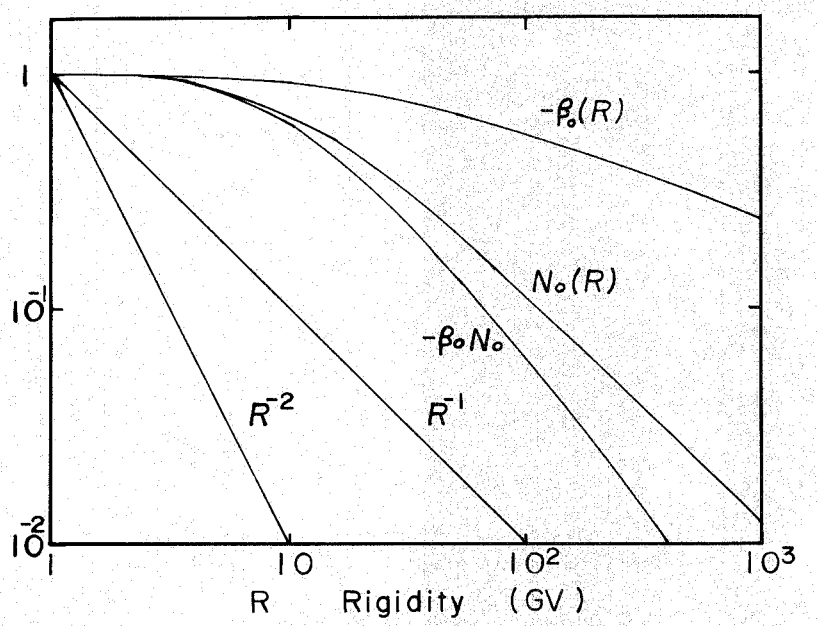

Fig.20. Rigidity dependence of barometer coefficient $\beta_o(R, p)$, neutron monitor intensity $N_o(R, p)$ and product $\beta_o(R, p)N_o(R, p)$ at sea level used in the numerical calculation. R^{-1} and R^{-2} are also plotted. The symbol p is abbreviated in the figure.

The quantity $\delta j/j_o$ represents the intensity variation of the primary cosmic radiation. We specify its precise dependence on the rigidity in the following form:

$$\frac{dJ(R)}{J_o(R)} = \begin{cases} AR^{-\gamma} & for \quad R \leq R_u \\ 0 & for \quad R > R_u \end{cases} \tag{7.15}$$

where R_u is the lower cutoff rigidity.

The calculations of α_γ have been performed as a function of the power exponent γ. Thus obtained values are plotted in Fig. 21, where the lower cutoff rigidity R_u=40GV is assumed. In practice, the computations have been carried out by using eq. (7.13) and eq. (7.14) independently, and the results of both calculations are compared to test the accuracy of computation. Cutoff rigidity R_c's are taken as 1,1.5, 2, 3, 5 and 7 GV.

Figure 22 represents the rigidity dependence of the observed α_γ, together with the theoretical curve of γ=1.7. Points A_2, B_1, and B_3 corresponding to the solar quiet period are found near the curve of γ=1.7. To compute the quantity α_γ when the solar activity is high, it is urgently necessary to derive the observational rigidity dependence of the barometer coefficient and the neutron intensity.

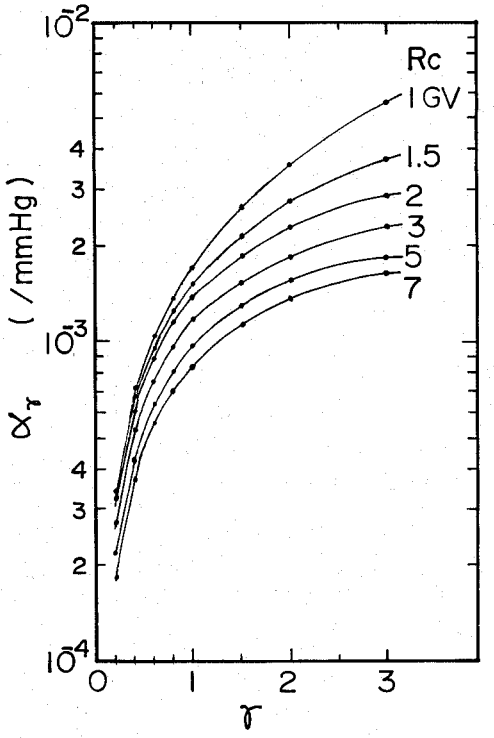

Fig.21. Results of numerical calculation of eq. (7.14). Where primary variation spectrum is assumed as $\delta J/J_0 \propto R^{-\gamma}$ ($R \leq 40GV$) and $\delta J/J_0 = 0 (R > 40GV)$. Cutoff rigidity Rc's sre taken as 1, 1.5, 2, 3, 5 and 7 GV.

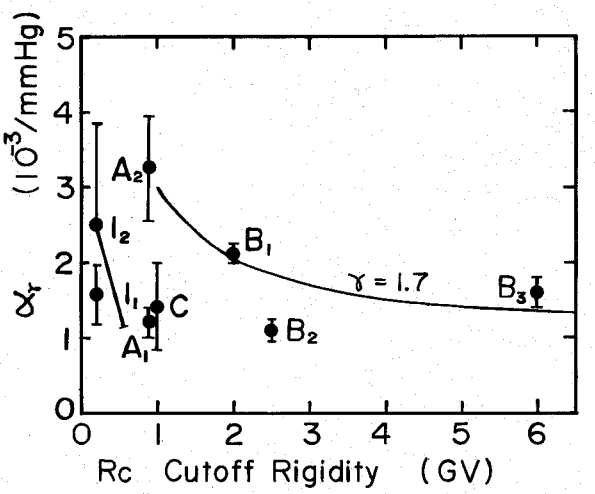

Fig.22 Distribution of α_γ are plotted in absolute value. The abscissa is the cutoff rigidity where the neutron monitor is located, or the mean rigidity at several stations. The curved line represents the distribution of α_γ, which is the result of numerical calculation of eq. (7.14), where $\gamma = 1.7GV$ is assumed.
A_1 and A_2 (Average of eight high latitude stations):Kusunose (1984).
I_1 and I_2 (Inuvik): Kusunose (1985)
B_1, B_2 and B_3 (Average of several stations):Bachelet *et al.* (1972).
C (Deep River): Carmichael and Peterson (1971).

8. Summary and Conclusion

The first objective of the present work is to examine the barometer coefficients for the cosmic ray neutron monitors located at high latitudes. When the atmospheric pressure is recorded accurately enough for performing the barometric correction, we must decide that value of the barometer coefficient is the most appropriate to the barometric correction.

Section 2 contains the description of two types of neutron monitors, IGY and NM64.

In Section 3, we describe the method of spherical harmonic analysis for organizing a number of the data observed all-round the world. As the results of analysis, several examples of three dimensional representation of the cosmic ray intensity variation are presented.

In Section 4, we discuss the fundamental problem of the atmospheric effects on the counting rates of the neutron monitors. Most of these, the temperature effects are ignitable, because the effects are estimated to be small enough.

Section 5 deals with the examination of the barometer coefficient. The barometer coefficients used for the high latitude neutron monitors are evaluated basing on the spherical harmonic analysis. As is shown in Fig. 13, most of the barometer coefficients determined by means of this analysis show much better self-consistent with respect to the same atmospheric depth. New coefficients are listed in Table 4 and their differences from old ones are discussed.

In Section 6, we discuss a possible solar cycle variation of the barometer coefficients, that is the second objective of the present work. The solar cycle variation of barometer coefficient has been clarified by analyzing the data observed for twelve years by means of the same method as applied in the previous sections. The observed data are shown in Fig. 14. The absolute value of the barometer coefficient is positively correlated with the cosmic ray intensity ; the fractional variation of the barometer coefficient is found to be in the range of 0.1%～0.4%, when the cosmic ray neutron intensity variation is as large as 1 %.

The year-to-year variation rate of the barometer coefficient is larger in the solar quiet period than that in the solar active period. The difference in the variation rate may be attributed to the primary spectrum variation caused by the solar modulation.

In Section 7, an analysis is performed on the quantitative relation between the barometer coefficient and the cosmic ray primary spectrum. Using the rigidity spectra of the barometer coefficient and the sea level neutron intensity, the dependence of the barometer coefficient on the spectrum of primary cosmic rays is computed. The result shows clearly that the year-to-year variation rate of the barometer coefficient is determined by the changes of both the cutoff rigidity and the primary comic ray spectrum.

Acknowledgements

I thank Drs. N. Ogita, S. Yoshida and M. Wada for their continuous supports and helpful suggestions throughout the present work. I also thank Drs. I. Kondo, M. Kodama and Y. Inoue

for their valuable suggestions and careful readings of the manuscript. I am indebted to the members of the Department of Physics and Department of Information Science, Faculty od Science, Kochi University. Computer works were performed by using FACOM computers at the Computation Center of the Institute of Physical and Chemical Research, and the Data Processing Center of Kochi University.

References

Agrawal, S. P., S. K. Ray, and U. R. Rao : Multiplicity measurements at Ahmedabad, Proc. 11th Int. Conf. on Cosmic Rays, Budapest 1969, *Acta Physica Academiae Scientiarum Hungaricae*, **29**, Suppl. 2, 597 - 600 (1970).

Bachelet, F., P. Balta, E. Dyring, and N. Iucci : On the multiplicity effect in a standard cosmic-ray neutron monitor, *Nuovo Cimento*, **31**, 1126 - 1130 (1964).

Bachelet, F., P. Balata, E. Dyring, and N. Iucci : Attenuation coefficients of the cosmic-ray nucleonic component in the lower atmosphere, *Nuovo Cimento*, **35**, 23 - 35 (1965).

Bchelet, F., N. Iucci, G. Villoresi, and N. Zangrilli : The cosmic-ray spectral modulation above 2 GV, IV. The influence on the attenuation coefficient of the nucleonic component, *Nuovo Cimento*, **11B**, 1 - 12 (1972).

Belov, A. V., and L. I. Dorman : Dependence of cosmic ray barometer effect on primary variation spectrum, *Proc. 16th Int. Cosmic Ray Conf., Kyoto*, **4**, 310 - 314 (1979).

Bercovitch, M. : Atmospheric effects on cosmic ray monitors, *Proc. Int. Conf. on Cosmic Rays, Calgary*, Part A, 269 - 344 (1967).

Blomster, K. A., and P. J. Tanskanen : The influence of snow and water on the different multiplicities as observed in a neutron monitor NM-64 in Oulu, Proc. 11th Int. Conf. on Cosmic Rays, Budapest 1969, *Acta Physica Academiae Scientiarum Hungaricae*, **29**, Suppl. 2, 627 - 630 (1970).

Brunberg, E. A., and A. Datner : Experimental determination of electron orbits in the field ofa magnetic dipole, Part II, *Tellus*, **5** (1953) 269 - 292.

Carmichael,H. : Cosmic Rays, *IQSY Instruction manual*, No. 7, IQSY Secretariat, London (1964); Cosmic Rays (Instruments), *Annals of the IQSY*, **1**, MIT Press, Cambridge, 178 - 197 (1968).

Carmichael, H., M. Bercovitch, M. A. Shea, M. Magidin, and R. W. Peterson : Attenuation of neutron monitor radiation in the atmosphere, Proc. 10th Int. Conf. on Cosmic Rays, Calgary 1967, *Can. J. Phys.*, **46**, S1006 - S1013 (1968).

Carmichael, H., and M. Bercovitch : V. Analysis of IQSY cosmic-ray survey measurements, *Can. J. Phys.*, **47**, 2073 - 2093 (1969).

Carmichael, H., and R. W. Peterson : Dependence of the neutron monitor attenuation coefficient on atmospheric depth and on geomagnetic cutoff in 1966 and in 1970, *Proc. 12th Int. Cosmic Ray Conf., Hobart*, **3**, 887 - 892 (1971).

Compton, A. H., E. O. Wollan, and R. D. Bennet : A precision recording cosmic-ray meter, *Rev. Sci. Instr.*, **5**, 415 - 422 (1934).

Dorman, L. I. : *Cosmic Ray Variations*, Transl. Tecn. Doc. Liaison Office, Wright-Patterson Air Force Base in USA (1958).

Dyring, E., and B. Sporre : The latitude effect of the neutron multiplicity as detected by a shipborne neutron monitor, *Ark. Geofys.*, **5**, 67 - 77 (1966a).

Dyring, E., and B. Sporre : Multiplicity measurements on the Uppsala IGY-neutron monitor, *Ark. Geofys.*, **5**, 79 - 85 (1966b).

Forman, M. A. : Neutron monitor mass absorptiom coefficients at Chicago and Climax during the solar cycle 19 (1954), *J. Geophys. Res.*, **70**, 2469 - 2473 (1965).

Fowler, I. L. : Very large boron trifluoride proportional counters, *Rev. Sci. Instr.*, **34**, 731 - 739 (1963).

Fujii, Z., M. Kodama, and M. Wada : The influence of gate time width on the multiple neutron distributions observed in the NM64 cosmic ray neutron monitor, *Sci. Papers Inst. Phys. Chem. Res.*, **66**, 1 - 9 (1972).

Gauss, C. F. : Allgemeine Theorie des Erdmagnetismus, *Resultate aus den Beobachtungen des Magnetischen Vereins im Jahre 1838*, (Herausgeber von C. F. Gauss und W. Weber), Weidmann, Leipzig, 1 - 57 (1839).

Griffiths, W. K., C. V. Harman, C. J. Hatton, and P. Ryder : Studies of the barometric coefficients of IGY and NM-64 neutron monitors, *Proc. Int. Conf. Cosmic Rays, London*, 475 - 477 (1965).

Griffiths, W. K., C. J. Hatton, P. Ryder, and C. V. Harman : The variation of the barometer coefficient of the Leeds neutron monitor during the solar cycle 1954 - 1965, *J. Geophys. Res* ., **71**, 1895 - 1898 (1966).

Griffiths, W. K., G. V. Harman, C. J. Hatton, P. L. Marsden, and P. Ryder : The intensity variations of selected multiplicities in the Leeds NM-64 neutron monitor. *Can. J. Phys.*, **46** , S1044 - S1047 (1968).

Harman, C. V., and C. J. Hatton : Contributions to the counting rate and the temperature dependence of neutron monitors, *Can. J. Phys.*, **46**, S1052 - S1056 (1968).

Hatton, C. J. and H. Carmichael: Experimental investigation of the NM-64 neutron monitor, *Can. J. Phys.*, **42**, 2443 - 2472 (1964).

Hatton, C. J. : The neutron monitor, *Progress in Elementary Particle and Cosmic Ray Physics*, (Ed. J. G. Wilson, and S. A. Wouthuysen), **10**, North-Holland Pub. Co., Amsterdam, 3 - 100 (1971).

Hughes, E. B., and P. L. Marsden : Response of a standard IGY neutron monitor, *J. Geophys. Res.*, **71**, 1435 - 1444 (1966).

Inoue, A., M. Wada, and I. Kondo : Asymptotic direction in 1975, *Cosmic Tables*, No. 1, World Data Center C2 for Cosmic Rays, Institute of Physical and Chemical Research, Tokyo (1983).

Ishii, C. : Nishina Ichigata Uchusenkei no Shoseino (in Japanese), *Riken Iho*, **23**, 535 - 545 (1944).

Jory, F. S. : Selected cosmic-ray orbits in the earth's magnetic field, *Phys. Rev.*, **103**, 1068 - 1075 (1956).

Kaminer, N. S., S. F. Ilgch, T. S. Khadakhanova : Temperature effect of the cosmic ray neutron component, *Proc. Int. Conf. Cosmic Rays, London*, **1**, 486 - 488 (1965).

Kamphouse, J. L. : Correlation of neutron monitor pressure coefficient and the solar cycle, *J. Geopys. Res.*, **68**, 5608 - 5610 (1963).

Kawasaki, S. : On the anomalous time variation in cosmic-ray neutron intensity caused by atmospheric pressure deviation due to high wind (in Japanese, with abstract in English), *Riken Hokoku*, **42**, 60 - 67 (1966).

Kawasaki, S.: On the anomalous barometer coefficient of cosmic-ray neutron monitor at Mt. Norikura, *Sci. Paper Inst. Phys. Chem. Res.*, **66**, 25 - 32 (1972).

Kawasaki, S. : Free air pressure reduced from radiosonde data for the correction of cosmic ray barometer effect, *Proc. 16th Int. Cosmic Ray Conf., Kyoto*, **4**, 263 - 265 (1979).

Kawasaki, S., K. Imai, and M. Wada : The cosmic ray intensities observed by Mt. Norikura neutron monitor, 1968 - 1980, *ICR-Report-109-83-03*, Inst. Cosmic Ray. Res., Univ. Tokyo (1983).

Kawasaki, S., and M. Wada : Estimation of free air pressure from radiosonde data for the correction of cosmic ray barometer effect, *Proc. 18th Int. Cosmic Ray Conf., Bangalore*, **3**, 473 - 475 (1983).

Kent, D. B., H. Coxell, and M. A. Pomerantz : Latitude survey of the frequency of multiple events in an airborne neutron monitor, *Can. J. Phys.*, **46**, S1082 - S1086 (1968).

Kodama, M., and A. Inoue : Differential rigidity response of different multiplicities in the NM-64 neutron monitor, Proc. 11th Int. Conf. Cosmic Rays, Budapest 1969, *Acta Physica Academiae Scientiarum Hungaricae*, **29**, Suppl. 2, 577 - 581 (1970).

Kodama, M., and A. Inoue : Availability and limitation of multiplicity measurements in the NM-64 neutron monitor at Syowa Station, Antarctica, *Japanese Antarctic Research Expedition Sci. Rep.* Ser. A, No. 9, Polar Research Center, National Science Museum (1970).

Kusunose, M., and M. Wada : Characteristics of Nishina-type ion chamber (in Japanese, with summary in English), *Riken Hokoku*, **45**, 93 - 104 (1969).

Kusunose, M., and M. Kodama : The effect of high wind on the correction of cosmic-ray intensity for barometric pressure at Syowa Station, Antarctica (in Japanese, with summary in English), *Riken Hokoku*, **48**, 121 - 127 (1972).

Kusunose, M., N. Ogita, and S. Yoshida : Examination of the barometric coefficients of neutron monitor data, *Proc. 17th Int. Cosmic Ray Conf., Paris*, **10**, 281 - 284 (1981).

Kusunose, M. : A solar cycle variation in the barometer coefficients of high latitude neutron monitors, *J. Phys. Soc. Japan*, **53**, 4488 - 4498 (1984).

Kusunose, M.: Year-to-year variation in the barometer coefficient of cosmic ray neutron monitor located at high latitude, *Mem. Fac. Sci. Kochi Univ.*, **5**, Ser. B, 15 - 20 (1985).

Kusunose, M., and N. Ogita : On the solar cycle variation in the barometer coefficients of high latitude neutron monitors, *Proc. 19th Int. Cosmic Ray Conf., La Jolla*, **5**, 305 - 308 (1985).

Lapointe, S. M., and D. C. Rose : A statistical analysis of the barometer coefficients for cosmic-ray intensities, *Can. J. Phys.*,**40**, 687 - 697 (1962).

Lockwood, J. A., and P. Singh : Cosmic-ray modulation during Forbush decrease in 1968 - 1969, Proc. 11th Int. Conf. on Cosmic Rays, Budapest 1969, *Acta Physica Academiae Scientiarum Hungaricae*, **29**, Suppl. 2, 319 - 325 (1970).

Lust, R., and J. A. Simpson : Document 5356, A. D. I. Auxiliary Publications Project, Library of Congress, Washington, D. C. (1957).

Malmfors, K. G. : Determination of orbits in the field of a magnetic dipole with applications to the theory of the diurnal variation of cosmic radiation, *Arkiv Mat., Astr. Fys.*, **32A**, 1 - 64 (1945).

Martinelle, S. : Air pressure dependence of cosmic ray intensity - Methods and results of a statistical analysis on neutron monitor data, *Tellus*, **20**, 1 - 197 (1968).

McCracken, K. G., and D. H. Johns : The attenuation length of the high energy nucleonic component of cosmic radiation near sea level, *Nuovo Cimento*, **13**, 96 - 107 (1959).

McCraken, K. G., U. R. Rao, B. C. Fowler, M. A. Shea, and D. F. Smart : Cosmic ray tables - Asymptotic directions, variational coefficients and cutoff rigidities, *IQSY Instruction Manual*, No. 10, IQSY Committee, London (1965).

Myssowsky, L., and L. Tuwim : Ungeselmässige Intensitätsschwankungen der Höhen- strahlung in geringer Seehöhe. *Phys. Z.*, **39**, 146 - 150 (1926).

Nagashima, K., S. P. Duggal, and M. A. Pomerantz : Cosmic ray anisotropy in three-dimensional space, *Planet. Space Sci.*, **16**, 29 - 46 (1968).

Nagashima, K. : Three dimensional cosmic-ray anisotropy in interplanetary space, Part I - Formulation of cosmic-ray daily variation produced by axis-symmetric anisotropy, *Rep. Ionos. Space. Res. Japan*, **25**, 189 - 211 (1971).

Ogita, N., S. Yoshida, T. Niikura, and M. Wada : Reexamination of the pressure corrected neutron monitor data, *Proc. 13th Int. Cosmic Ray Conf. Denver*, **2**, 831 - 834 (1973).

Raubenheimer, B. C., and P. H. Stoker : Various aspects of the attenuation coefficients of a neutron monitor, *J. Geophys. Res.*, **79**, 5069 - 5076 (1974).

Shimizu, I., Y. Yajima, Y. Uno, K. Sato, and T. Matsuda : Kiatsu no Toriireguchi (in Japanese), *Tenki*, **14**, 147 - 150 (1967).

Simpson, J. A., W. H. Fonger, and S. B. Treiman : Cosmic radiation intensity-time variations and their origin, I. Neutron intensity variation method and meteorological factors, *Phys. Rev.*, **90**, 934 - 950 (1953).

Simpson, J. A. : *Annals of the International Geophysical Year*, Pergamon Press, London, **4** (1957).

Smirnov, V. S., and V. T. Ustinovich : Threshold rigidities and coupling constants of a neutron supermonitor and a multiplicity meter, Proc. 11th Int. Conf. on Cosmic Rays, Budapest 1969, *Acta Physica Academiae Scientiarum Hungaricae*, **29**, Suppl. 2, 635 - 637 (1970).

Störmer, C. : *The polar aurora*, Claredon Press, Oxford (1955).

Yoshida, S., S.-I. Akasofu, N. Ogita, and K. Outi : Spherical harmonic analysis of worldwide cosmic ray variation during geomagnetic storms, *J. Geophys. Res.*, **76**, 1 - 12 (1971).

Manuscript received : September 30, 1997
Published : December 25, 1997